DTIC FILE COPY

②

REPORT DOCUMENTATION PAGE

READ INSTRUCTIONS
BEFORE COMPLETING FORM

1. REPORT NUMBER	2. GOVT ACCESSION NO.	3. RECIPIENT'S CATALOG NUMBER
R/D 5027-OH -01		

4. TITLE (and Subtitle)	5. TYPE OF REPORT & PERIOD COVERED
COLLOIDAL ASSEMBLIES EFFECT ON CHEMICAL REACTIONS	FINAL AUGUST 1985 - DECEMBER 88
	6. PERFORMING ORG. REPORT NUMBER

7. AUTHOR(s)	8. CONTRACT OR GRANT NUMBER(s)
Ezio PELIZZETTI	DAJA 45-85-C-0023

9. PERFORMING ORGANIZATION NAME AND ADDRESS	10. PROGRAM ELEMENT, PROJECT, TASK AREA & WORK UNIT NUMBERS
Università di Torino Via Verdi 8, 10125 Torino, Italy	

11. CONTROLLING OFFICE NAME AND ADDRESS	12. REPORT DATE
	DECEMBER 1988
	13. NUMBER OF PAGES
	29

14. MONITORING AGENCY NAME & ADDRESS(if different from Controlling Office)	15. SECURITY CLASS. (of this report)
	15a. DECLASSIFICATION/DOWNGRADING SCHEDULE

16. DISTRIBUTION STATEMENT (of this Report)

'PROVED FOR PUBLIC RELEASE - DISTRIBUTION UNLIMITED

17. DISTRIBUTION STATEMENT (of the abstract entered in Block 20, if different from Report)

DTIC
ELECTE
FEB 23 1989

18. SUPPLEMENTARY NOTES

19. KEY WORDS (Continue on reverse side if necessary and identify by block number)

COLOIDS, MICELLES, MICROEMULSIONS, SURFACTANTS, OXIDATION, PHOTOCATALYSIS, SEMICONDUCTORS, DEGRADATION, MINERALIZATION, HALOAROMATIC COMPOUNDS, REACTION MECHANISMS, KINETICS.

20. ABSTRACT (Continue on reverse side if necessary and identify by block number)

The influence that organized assemblies (micelles, microemulsions) and semiconductor colloids exhibits on chemical reactions has been investigated.
In particular electron transfer reactions induced by light in the presence of semiconductor particles have been shown to completely degrade potentially dangereous compounds.

DD FORM 1473 EDITION OF 1 NOV 65 IS OBSOLETE
1 JAN 73

AD-A205 519

89 2 22 043

The photodegradation catalyzed by TiO_2 particles of phenol, p-alkylphenols and ethoxylated non-ionic surfactants derived from p-nonylphenol has been investigated by carrying out the experiments in different experimental conditions. Intermediate formation has been followed through HPLC analysis. CO_2 evolution as well as DOC and POC measurements confirm the complete degradation.

Similarly, the photocatalytic degradation of 2,4,5-trichlorophenoxyacetic acid (2,4,5-T) and 2,4,5-trichlorophenol on TiO_2 led to complete mineralization into CO_2 and HCl. In the degradation of 2,4,5-T several intermediates were detected by GC-MS and a scheme for the photodegradation pathways was formulated.

The photodegradation process in the presence of semiconductors has been shown to be efficient also with persistent and sparingly soluble haloaromatic compounds such as DDT, dioxins, PCB's. The photoreactions at semiconductors of some non-halogenated solvents, i.e. cellosolves, have been shown to effectively degrade also these water-miscible contaminants.

Finally, herbicides of the s-triazine family (e.g. atrazine) have been degraded even at ppb levels.

Since the proposed photodegradative mechanism involves the intervention of $OH^{\cdot}$ radicals, Fenton's reagent (Fe^{2+} + H_2O_2) was investigated as possible reagent for halophenols degradation. The mineralization of these compounds was in fact found to occur and the effect of the concentration of Fe^{2+}, Fe^{3+}, $HClO_4$ was investigated.

Microemulsions are transparent dispersion of oil-in-water (O/W) or water-in-oil (W/O) in the presence of a surfactant and a cosurfactant. These aggregates can bring reactants together or to bring them apart and solubilize large amounts of sparingly water soluble compounds.

The kinetics and equilibrium of the formation of the ground state charge transfer complex between durene and chloranil was investigated in O/W microemulsions.

Electron transfer reactions between benzenediols and $IrCl_6^{2-}$ and between $IrCl_6^{3-}$ and 12-tungstocobaltate(III) were investigated over a wide range of microemulsion composition (from O/W to W/O). A three pseudo-phase model accounting for the observed rate constants was proposed.

Electron transfer reactions have been investigated also in cationic micellar systems and a model for the kinetics has been proposed.

Due to the importance of the solubilization of sparingly soluble organic compounds in micellar aggregates, the interaction of a series of differently substituted phenols with anionic micelles has been investigated. Group contribution to the binding constants has been evaluated for several substituents and their additivity

has been demonstrated.

The complexing and extracting properties of a functionalized surfactant family (4-alkylamidosalycilic acids) were investigated. The acid-base properties of the surfactant ligands, the partitioning and the kinetics of complex formation in the presence of non-ionic micelles were studied. The proper conditions for an efficient iron(III) complexation and extraction were determined.

DTIC
COPY
INSPECTED
1

Accesion For

NTIS	CRA&I	☑
DTIC	TAB	☐
U...		☐
J...		

A-1

AD

COLLOIDAL ASSEMBLIES EFFECT ON CHEMICAL REACTIONS

Final Technical Report

by

Ezio PELIZZETTI

December 1988

United States Army

EUROPEAN RESEARCH OFFICE OF THE U.S. ARMY

London England

CONTRACT NUMBER DAJA 45-85-C-0023

Università di Torino, Italy

Illustrations, Tables

LIST OF PUBLICATIONS

1) V.Augugliaro, L.Palmisano, A.Sclafani, C.Minero, and
   E.Pelizzetti, "Photocatalytic Degradation of Phenol in Aqueous
   Titanium Dioxide Dispersions", Toxicol.Environ.Chem.,
   1988, 16, 89.

2) M.Barbeni, M.Morello, E.Pramauro, E.Pelizzetti, M.Vincenti,
   E.Borgarello, and N.Serpone, "Sunlight Photodegradation of
   2,4,5-Trichlorophenoxyacetic Acid and 2,4,5-Trichlorophenol
   on TiO_2. Identification of Intermediates and Degradation
   Pathway", Chemosphere, 1987, 16, 1165.

3) E.Pelizzetti, M.Borgarello, C.Minero, E.Pramauro, E.Borgarello,
   and N.Serpone, "Photocatalytic Degradation of Polychlorinated
   Biphenyls in Aqueous Suspensions of Semiconductors Irradiated
   with Simulated Solar Light", Chemosphere, 1988, 17, 499.

4) R.Borello, C.Minero, E.Pramauro, E.Pelizzetti, N.Serpone, and
   H.Hidaka, "Photocatalytic Degradation of DDT Mediated in Aqueous
   Semiconductor Slurries by AM1 Simulated Sunlight",
   submitted.

5) E.Pelizzetti, V.Maurino, C.Minero, E.Pramauro, O.Zerbinati,
   and M.L.Tosato, "Photocatalytic Degradation of s-Triazine
   Pesticides", in preparation.

6) C.Minero, V.Maurino, L.Campanella, C.Morgia, and E.Pelizzetti,
   "Photodegradation of 2-Ethoxy- and 2-Butoxyethanol in the
   Presence of Semiconductor Particles or Organic Conducting
   Polymer", submitted.

7) E.Pelizzetti, V.Maurino, C.Minero, A.Sclafani, H.Hidaka,
   and N.Serpone, "Photocatalytic Degradation of Nonylphenol
   Ethoxylated Surfactants", submitted.

8) E.Pelizzetti, E.Pramauro, C.Maurino, N.Serpone, and E.Borgarello,
   "Photodegradation of Organic Pollutants in Aquatic Systems
   Catalyzed by Semiconductors", in "Photocatalysis and Environment",
   M.Schiavello ed., Kluwer Acad. Publ., Dordrecht, 1988, p. 469.

9) E.Pelizzetti, E.Pramauro, C.Minero, and N.Serpone,
   "Sunlight Photodegradation of Organic Pollutants Catalyzed
   by Semiconductor Materials", submitted.

10) M.Barbeni, C.Minero, E.Pelizzetti, E.Borgarello, and N.Serpone,
    "Chemical Degradation of Chlorophenols with Fenton's Reagent",
    Chemosphere, 1987, 16, 2225.

11) P.P.Infelta, R.Graglia, C.Minero, and E.Pelizzetti,
"Ground State Charge Transfer Complexes in O/W Microemulsions",
Coll.Surfaces, 1987, *28*, 289.

12) C.Minero, E.Pelizzetti, and E.Pramauro, *"Electron Transfer
Reactions in Microemulsions*: Oxidation of Benzenediols by
Hexachloroiridate(IV)"*, Langmuir, 1988, *4*, 101.

13) C.Minero, E.Pramauro, and E.Pelizzetti, "Reaction Kinetics
as a *Probe for* the Structuring of Microemulsions",
Coll.Surfaces, in press.

14) E.Pelizzetti, E.Pramauro, and C.Minero, "Kinetics and Reactivity
in O/W Microemulsions", Ann.Chim.(Rome), 1987, *77*, 127.

15) C.Minero, E.Pramauro, and E.Pelizzetti, "Generalized Two-Pseudo-
phase Model for Ionic Reaction Rates and Equilibria in Micellar
Systems. Hexachloroiridate(IV)-Iron(II) Electron Transfer in
Cationic Micelles", J.Phys.Chem., 1988, *92*, 4670.

16) E.Pramauro, C.Minero, G.Saini, R.Graglia, and E.Pelizzetti,
"Partitioning of Phenols between Water and Anionic Micelles.
Correlation with the Octanol-Water System", Anal.Chim.Acta,
1988, *212*, 171.

17) E.Pramauro, C.Minero, and E.Pelizzetti, "Use of Amphiphilic
Ligands in Chemical Separations", in "Use of Ordered Media
in Chemical Separations", W.L.Hinze and D.W.Armstrong eds.,
ACS Symp. Ser., 1987, *342*, 152.

18) F.P.Cavasino, C.Sbriziolo, E.Pelizzetti, and E.Pramauro,
"Kinetic and Equilibrium Studies of Complex Formation between
Iron(III) and 4-Alkylamido-2-hydroxybenzoic Acids in Aqueous
Nonionic Micellar Media", J.Phys.Chem., in press.

19) E.Pramauro, E.Pelizzetti, C.Minero, E.Barni, P.Savarino, and
G.Viscardi, "Properties and Applications of Amphiphilic and
Hydrophobic Ligands", Ann.Chim.(Rome), 1987, *77*, 209.

Participating scientific personel

Edmondo PRAMAURO   Associate Professor

Claudio MINERO   Associate Researcher

CONTENT

I. PHOTODEGRADATION OF ORGANIC COMPOUNDS BY VISIBLE LIGHT

Semiconductor particles have been proved to be active ca
talysts in organic transformations induced by light.
Since Chloroaromatic derivatives are compounds of relevant
concern because same of them are bioaccumulative and persi-
stent in the environment and also extremely toxic, their be
havior under solar light has been investigated.
In fact microbial degradation and naturally occurring hydro
lysis require long periods; direct photodegradation requires
high energy photons often leading to incomplete decomposi -
tion and, in some cases, to the formation of dangerous pro-
ducts.

Heterogeneous photo-assisted catalytic degradation by
means of semiconductor particles has been applied to a va-
riety of aromatic compounds.

The efficiency of these photocatalyzed reactions depends
on many factors and mainly on the nature of the semiconduc-
tor. Figure 1 shows the results of light exposure of aerated
aqueous solutions of 3,4 dichlorophenol in the presence of
2 g/l of various semiconductor suspension, at constant pH
and temperature. The spectral distribution of irradiation
(from a Solarbox lamp) in the experimental range 310-830 nm
corresponded to AM1 solar illumination.
The experiments concerning phenol and 3,4,5-trichlorophenoxy-
acetic acid degradation were carried out mainly with TiO_2
as photocatalyst.

I.1. Phenol

A typical experiment of phenol photocatalytic degradation
is reported in Figure 2 where also the intermediate benzene-
diol (quinol and catechol, identified by LC) concentration
is shown.
The salient features experimentally observed can be summari-
zed as follows:
- the photodegradation is pH dependent and the highest photo
  reactivity is observed in the alkaline region;
- there is not degradation in absence of oxygen;
- the presence of massive amount of Cl^- negatively affects
  the degradation rate;
- the degradation rate is negatively affected by the initial
  phenol concentration;
- the reflectance spectrum of TiO_2 is not affected by the
  phenol adsorbed from a solution at pH 3, whilst it is af-
  fected when the phenol is adsorbed from a solution at pH
  13, anatase being more photoactive than rutile;

- intermediate compounds are detected which are unstable and photodegraded.

An indication of the catalytic nature is obtained from the sunlight experiments, for which it was observed that the reaction proceeded for months without showing any decline. Moreover a rough calculation of the turnover number, molecu les converted/(sites·h), gives a figure of about 200, show- ing that the surface sites are renewed 200 times in one hour. This calculation was made considering an initial rate of phenol photodegradation of 60 mg l^{-1} h^{-1}, $5 \cdot 10^{14}$ surface OH^- sites/cm^2 and that for the complete phenol oxidation 28 electrons are required.

It may be safely assumed that in the alkaline slurry the surface of TiO_2 is fully covered with water molecules and with OH^- groups; in a somewhat similar situation it has been demonstrated that OH^- groups and water molecules are rough- ly in a 1:1 ratio. The OH^- groups will likely exhibit a ran- ge of acid-base strength, according to the nature of the si tes in which they are accomodated.

As far as the rate determining step of the process is concerned, it can be excluded any influence of mass transfer rate limitation to the solid-liquid interface. It would ari se if the phenol and oxygen concentrations on the TiO_2 sur- face were practically zero. By calculating the ratio bet- ween the maximum mass transfer rate and the reaction rate, it comes out to be of the order of magnitude of 10^3. This consideration indicates that the slow step in the phenol pho todegradation process concerns the surface catalytic reac- tion because the liquid-solid mass transfer rate offers a negligible resistance.

We may therefore state that the photodegradation reaction occurs between the reactants both adsorbed on the TiO_2 sur- face. These adsorbed species as well as others present on the surface like OH^- will be involved in the reaction. The- refore the extent and the rate of the reaction is affected by the nature of the interaction between the reactants with the surface as well as by the electronic properties of the irradiated semiconductor.

The reflectance spectra of TiO_2 on whose surface phenol from a pH 13 solution, i.e. phenate ion, is adsorbed, clear ly indicate that this species interacts with the surface forming a complex able to absorb visible radiation, while the phenate ions solution is photoactive in the UV region of the spectrum only.

It is not straighforward to define how the phenate ions are bonded to a surface fully covered by water molecules and OH^- groups. We may only observe that the complex formed with the surface has an energy content higher than the ener

gy level of the phenate ion in solution and therefore it is prone to undergo a chemical transformation.

As for the oxygen, a variety of more or less stable species were detected according to the amount of hydroxylation, although there is a widespread agreement that the primary species in oxygen photoadsorption, in conditions similar to those used is O_2^- . Moreover it has been observed that oxygen photoadsorption is enhanced by the presence of hydroxyl groups while the presence of Cl^- groups, decreasing the OH^- content, decreases also the oxygen photoadsorption.

Having in mind the above considerations and also that, in absence of oxygen, no phenol photodegradation occurs, a tentative reaction scheme can be proposed.

In a photocatalytic process the primary step is, of course, the photogeneration of pairs of electrons and holes which must be trapped to avoid recombination (charge separation):

$$TiO_2 + h\nu \rightarrow TiO_2 + e(cb) + h(vb) \qquad (1)$$
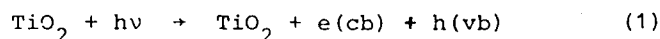
It is widely accepted that the hydroxyl groups are the likely traps for holes:

$$OH^- + h^+ \longrightarrow OH\cdot \qquad (2)$$

The possible destiny of $OH\cdot$ radicals can be described by the following reactions:

$$OH\cdot + OH\cdot \rightarrow H_2O_2 \qquad (3)$$

$$H_2O_2 \rightarrow H-O-O^- + H^+ \qquad (4)$$
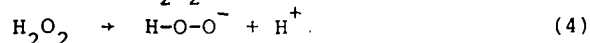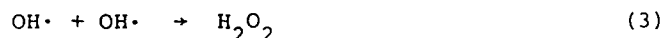
The peroxide ion is a well known oxidizing agent for organic substrates. In our case it must be also observed that, due to the fact that the surface phenate complex absorbs light at wavelength higher than that corresponding to the energy of the band gap of TiO_2, the complex itself may act as sensitizer according the following reaction:

$$C_6H_5O^- + h\nu \rightarrow C_6H_5O\cdot + e(cb, TiO_2) \qquad (5)$$
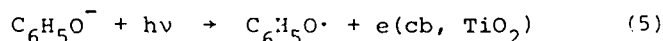
If this reaction takes place, then the phenate complex hastens the charge separation step and injects electrons to the con duction band of TiO_2.

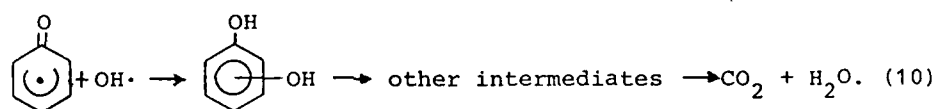The traps for electrons are adsorbed oxygen species accor ding to the following equations:

$$O_2(gas) \rightleftarrows O_2(ads) \qquad (6)$$

$$O_2(ads) + e^- \rightleftarrows O_2^-(ads) \qquad (7)$$
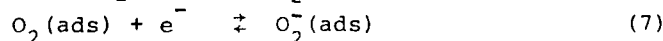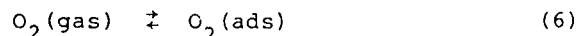
The superoxide species is unstable and reactive. It may evol
ve in several ways:

and/or:

$$O_2^-(ads) + OH\cdot \rightarrow HO_2^\cdot + O^-(ads) \qquad (8)$$

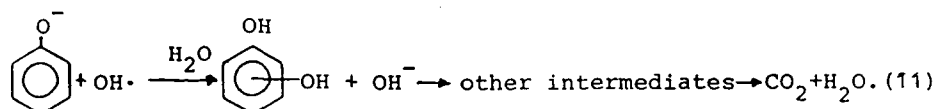$$O_2^-(ads) + H_2O \rightarrow OH^- + HO_2^\cdot \qquad (9)$$
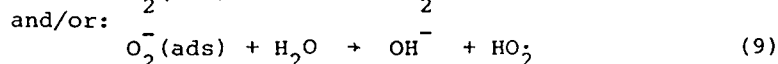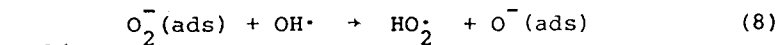
Thus as a consequence of the primary step of electrons and
holes trapping, several species are produced, which will be
involved in the reaction mechanism.

If the phenate ions act as sensitizer., thus forming ra-
dicals, these latter may likely evolve as follows:

$$\text{[benzene ring with O, } \cdot\text{]} + OH\cdot \rightarrow \text{[benzene ring OH]}-OH \rightarrow \text{other intermediates} \rightarrow CO_2 + H_2O. \quad (10)$$

In the phenate ion is still under an ionic form, the follow-
ing scheme may be proposed:

$$\text{[benzene ring O}^-\text{]} + OH\cdot \xrightarrow{H_2O} \text{[benzene ring OH]}-OH + OH^- \rightarrow \text{other intermediates} \rightarrow CO_2 + H_2O. \quad (11)$$

The scheme proposed accounts for the main findings and in
dicates also the reasons why the photodegradation is lower
in the acidic region. These reasons clearly are:
- the OH⁻ traps are much less in acidic medium than in the
  alkaline medium; therefore the charge separation step is
  less efficient;
- the reflectance spectra of TiO_2, treated with phenol from
  acidic solution do not show appreciable change, indicating
  that the adsorption of phenol is very scarce;
- the chemisorption of O_2 in acidic medium is lowered with
  respect to the alkaline medium.

All these reasons affect in a negative way the course of
the reaction in acidic medium. Finally it must be observed
that adding Cl⁻ to the dispersions lowers the activity for
the reasons already given. Of course this effect is much
more evident in the acidic medium than in the alkaline me-
dium where a very large amount of OH⁻ is present.

I.2. 2,4,5-Trichlorophenoxyacetic acid (2,4,5-7) and 2,4,5-
     Trichlorophenol (2,4,5-TCP)

As shown in Figure 1, chlorophenols can be photocatalyti-
cally degraded by semiconductor particles under visible light.
Because of its importance, the photocatalytic degradation

of 2,4,5-T has been investigated as well as that of 2,4,5-trichlorophenol which has been shown to be one of the major intermediate species.

Fig. 3a illustrates the complete degradation of 2,4,5-T and 2,4,5-TCP in aqueous suspensions of TiO_2 in the presence of air. Illumination ($\lambda \geq 340$ nm) of 1×10^{-4} M of 2,4,5-T and 2,4,5-TCP in air and in the presence of suspended titanium dioxide results in the rapid disappearance of the chlorinated organic compounds with the concomitant formation of Cl^- (Fig. 3b). The amount of Cl^- (ca. 3×10^{-4}M) and CO_2 formed confirms the complete mineralization of 2,4,5-T and 2,4,5-TCP. For example, 2×10^{-6} moles of 2,4,5-TCP gave 1.2×10^{-5} moles of CO_2, according to the stoichiometric equation (12):

$$HOC_6H_2Cl_3 \quad + \quad 11/2 \ O_2 \quad \xrightarrow[h\nu]{TiO_2} \quad 6CO_2 + 3HCl \qquad (12)$$
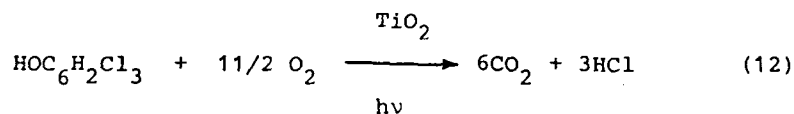
From the ratio between Cl^- formed and 2,4,5-T or 2,4,5-TCP degraded as a function of illumination time, it was observed that a difference exists between the degradation behaviour of the two chloro compounds; the ratio is 3 all along the reaction time for 2,4,5-TCP as expected from the stoichiometric decomposition (reaction 12). Such is not the case for the 2,4,5-T. In fact, only after 180 min of irradiation does the ratio between Cl^- formed and 2,4,5-T (1×10^{-4} M) consumed reach the value of 3, even though the total disappearance of 2,4,5-T from the solution occurs in less than 100 min (Figure 3).

According to these results, the degradation of 2,4,5-T, induced by irradiated TiO_2 dispersions, shows a very particular behaviour compared to the chlorophenols. In fact several intermediates were observed and identified by GC/MS after 20 min of irradiation under simulated AM1 conditions in aerated aqueous TiO_2 suspensions. The intermediate species were detected in a wide range of concentrations which showed to be crucial in proposing the several degradation pathways illustrated in Fig. 4. Of course, the identification of different intermeidates is dependent on the stability of the intermediate itself as some of these species undergo further facile oxidation. As a consequence, observation and identification of trace quantities of an unstable intermediate product, as well as the high concentration of a very stable intermediate species contribute to the formulation of a plausible degradation mechanism. Trace amounts of different reaction products were analyzed by taking into account the contribution of the impurities present initial-

ly in 2,4,5-T as supplied by the vendor. Parallel analyses were carried out on the products from the treatment of the intermediate species with diazomethane in order to decrease their polarity and to better identify these products by mass spectrometric techniques.

2,4,5-TCP (III) and 2,4,5-trichlorophenyl formate (IV) are the two major and longer lived intermediate products of the photodegradation of 2,4,5-T.
The $OH^\cdot$ (and $HO_2^\cdot$) radicals generated through sequence (1)-(9) can subsequently undergo a series of reactions with the 2,4,5-T, leading to the products summarized in the scheme illustrated in Fig. 4. The details of the mechanism are not yet entirely clear; however, it seems plausible, by simple analogy with the photodegradation of 4-chlorophenol, that repeated hydroxyl attack on the aromatic ring will lead to chloride radicals and eventually also to some semiquinonoid type radicals. The $Cl^\cdot$ radicals formed undergo subsequent reduction to Cl^- (reaction 13):

$$Cl^\cdot + e_{cb}^- \longrightarrow Cl^- \tag{13}$$

The semiquinone radicals formed can subsequently be oxidized (or can disproportionate), with the resulting benzoquinone undergoing further degradation via photocatalytic oxidation on TiO_2 as reported earlier. The photodegradation pathway reported in Fig. 4 is analogous to the mechanism proposed in the photochemical degradation of 2,4,5-T in the absence of TiO_2, except that polymer formation was observed instead of complete mineralization to CO_2 and HCl when TiO_2 is present. It is worth noting that the simple process of dehalogenation appears not to be significant in the photocatalyzed degradation of 2,4,5-T reported here.

Finally, the activity of the TiO_2 Degussa P-25 powder was tested for the photodegradation of 2,4,5-T by performing several runs with the same TiO_2 powder: 1.5×10^{-4} M of 2,4,5-T was irradiated for 60 min leaving 1.1×10^{5} M of non-decomposed substrate in solution. After this period, a fresh solution of 2,4,5-T was added and the photodegradation continued. This same cycle was repeated 11 times; the subsequent cycle was run for 120 min. At this point, the TiO_2 was washed with water, and then used again in the photodegradation process. From the results it is evident that the quantity of 2,4,5-T photodegraded with time is virtually constant and appears to have no consequence on the photo-activity of TiO_2. This is taken to suggest that no adsorption of final products and no modification of the surface occur.

I.3. Other haloaromatic Compounds

Since it was shown that TiO_2 exhibits the highest efficiency in the photodegradation of halophenols, it was chosen to investigate the decomposition of the series of chloroaromatic compounds listed in Table 1.

From these   data it is evident that the process can be applied to a wide variety of compounds, even when present at very low concentrations. The observed degradation half-life ($t_{1/2}$) seems to be only slightly affected by the increase in the halogen content as well as by the solubility of the compound; experiments have also demonstrated that photodegradation proceeds at a significant rate also under direct sunlight.

For compounds which are scarcely soluble in water, such as DDT, 3,3'-DCB or 2,7-DCDD, the experiments were performed after stirring the substrate dissolved in n-hexane with the semiconductor. Upon evaporation of the solvent the catalyst was suspended in aqueous media and irradiated.

In the case of DDT as well as dioxins and PCB's, the photocatalytic activity of some commercial powders of semiconductors was tested. As shown in Fig. 5, TiO_2 is the most active.

Interestingly for all these chlorinated compounds, which exhibit very long life in the environment, half-lives of 40-80 minutes are observed under photocatalytic conditions. However, for 2,7-dichlorodioxin only after 90 hours its concentration is reduced below 0.1 ppm from the initial concentration of 20 ppm (see Fig. 6) and even longer times are required for a complete mineralization.

I.4. Triazine herbicides

Triazines, compounds of general formula,

$$R_1, R_2 \diagdown N \text{—triazine ring—} X, N, R_3, R_4$$
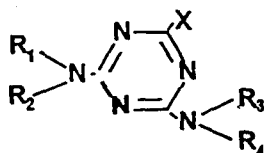
where $X = Cl$, OCH_3, SCH_3

and $R = H$, alkyl group,

represent a very popular class of herbicides used to control
broadleaf and grassy weeds in corn and also in sorghum,
sugarcane, pineapple and other crops. Because of the persis-
stence and the large and prolonged use, traces have been
found in groundwater, sometimes exceeding the admitted thre-
shold values.

The photocatalytic degradation of the compounds listed in
Table 2 has been demonstrated. It is noteworthy that the
process is still very efficient also at ppb levels (see Fig. 7).
Interestingly some s-triazine derivatives are stable to
photodegradation. Amino- and hydroxy substituted s-triazine
have in fact been detected after long irradiation times.
Work is in progress on this class of compounds.

I.5. NON-HALOGENATED SOLVENTS

Large volumes of solvent wastes are generated annually
and their disposal represents a problem of relevant environ-
mental concern. In many instances the organic solvents became
mixed with water and the resultant aqueous waste stream can
be treated in the framework of the several technologies impro-
ved in the last decade. Whereas photocatalytic mineralization
of low molecular weight halogenated solvents on TiO_2 particles
has been reported, little attention has been devoted to non-
halogenated solvents.

The photodegradation of two low molecular weight non-haloge-
nated solvents, namely 2-ethoxy- and 2-butoxyethanol, has then
been investigated. In addition to the method which uses semi-
conductor particles suspended in the aqueous waste, another
method with the use of organic conducting polymers has been
tested.

Conductive polymers can be obtained by polymerization of
monomers of suitable structure characterized by low redox
potential and/or high electronic affinity. Doping of the
obtained polymer with oxidizing or reducing agents yields a
polymer with an ionic structure formed respectively by the
cation of the polymer and the anion of the doping agent or
viceversa. According to the nature of the polymer and the nature
and concentration of the dopant, different values of cationic
or anionic conductivity are observed for the doped polymer.
Because of their polymeric nature, the preparation of a membrane
based on these compounds is quite simple and easy.

The degradation in the presence of TiO_2 particles is
depicted in Fig. 8, where in addition to the disappearance of
the 2-butoxyethanol, CO_2 evolution as well as DOC and POC
(Dissolved Organic Carbon and Particulate Organic Carbon,
respectively) are monitored.

Interestingly Fig. 9 reports the degradation in the presence
of organic conducting polymer, which has the advantage to be
easily removed from the solution.

Work is in progress on this matter.

I.6 NON-IONIC SURFACTANTS

The photocatalytic degradation of non-ionic nonylphenol ethoxylate surfactants has been investigated using TiO_2 particulate as photocatalyst. Degradation processes have been monitored through liquid chromatography, CO_2 evolution and DOC and POC measurements. Fig. 10-12 show the degradation process and the complete conversion to CO_2 has been demonstrated.

The degradation routes involve, in the early part of the process a competitive attack of hydroxy radicals on the ethoxy chain and on the aromatic ring, which can be rationalized in the framework of a kinetic model that we are developing. A reaction scheme, illustrated in Fig. 12, can be proposed. Work is in progress also in this matter.

I.7. REVIEWS. COMMENTS

   The photocatalytic processes leading to the degradation
of organic compounds have been reviewed extensively by the
present reporter (see ref. 8 and 9).
   Comparison with the several thermal and non-thermal
processes that can be used for treating organic wastes has
been attempted. In fact, some of these are difficult to apply
to water treatment and inasmuch as microbial degradation and
naturally occurring hydrolysis require long period, methods
involving the use of light can represent a valuable alternative.
These possibilities are listed in Table 3.
   The photocatalytic degradation method appears to be a
"soft" technique requiring low-temperature and low-pressure
conditions. In addition there are the following advantages:
(i) complete destruction of the organic contaminants is
generally observed in few hours
(ii) the process seems to avoid the formation of photocyclized
products
(iii) the process requires a non-expensivecatalyst with high
turnover and that can be supported in proper reactors
(iv) the process can be applied to contaminants present at
concentrations very low, even in the ppb range.
   In conclusion since the reaction conditions are mild and
the reaction times relatively short, the future challenge will
be from one side to have a better understanding of the funda+
mentals of photocatalytic processes and of the properties of
the catalysts and from the other side to demonstrate the
economic as well as the technical feasibility (proper and effi-
cient photoreactors) of the heterogeneous photocatalytic
treatment for the destruction of organic contaminants in
aquatic systems.

II. OXIDATIVE DEGRADATION OF ORGANIC COMPOUNDS

The degradation of organic pollutants by chemical oxidation affords an alternative route to the biological and natural routes, especially at high concentration of the contaminants. As shown in the previous section I the heterogeneous photocatalytic degradation of Chloro aromatic compounds proceeds through mechanism(s) in which OH· radical species may intervene in the reactions at irradiated aqueous slurries of TiO_2.

Similarly, Fenton's reagent ($Fe^{2+} + H_2O_2$) easily induces the degradation of chlorinated phenols if excess H_2O_2 is used and O_2 is present in the reaction mixture.

Fig. 13 depicts the decrease in concentration of differently mono substituted chlorophenols as a function of time. The results demonstrate that the 3-chlorophenol (3-CP) is rapidly degraded in the presence of a $Fe^{2+}/H_2O_2/O_2$ mixture; disappearance of the analogous 2-CP and 4-CP is slower under the same conditions. Concomitant with the degradation of these CP species, an equimolar amount of free chloride ions in solution was detected (Fig.13). A parallel experiment performed on the same reaction batch, but using HPLC techniques to detect the fate of the chlorophenols or its intermediates showed complete degradation of the aromatic ring. This implicates the occurrence of an oxidative process and not merely a simple dehalogenation substitution reaction.
Analogous results were obtained for the dichlorophenols and trichlorophenols under identical conditions. In Table 2 are summarized the times necessary (t/2) to reduce the initial concentration of the chlorophenols in solution by a factor of two. It should be pointed out that this t/2 parameter is a practical operational parameter that includes any (if any) induction period to the start of the degradation reaction and must not be confused with the $t_{1/2}$ kinetic parameter for the reaction of disappearance. This procedure allows us to compare, in practical terms, the times required for the total degradation of these contaminants, even though the mechanism(s) may or may not be identical.

It is intriguing to note (cf. Fig.13) that among the monochlorophenols, meta-chloro substitution induces a more rapid degradation than either of the ortho-chloro or para-chloro substitution. The differences in the rates of decomposition of these mono-chlorinated species is real. At higher $/HClO_4 /$, the degradation is considerably inhibited as clearly noted in Table 4, which also summarizes t/2 values with changes in $/HClO_4 /$. For the same $HClO_4$ concentration and for the same Fe^{2+}/H_2O_2 ratio, the 3,4-dichlorophenol (3,4-DCP) decomposes faster than any of the other compounds studied. In all cases, the stoichiometric quantity of free Cl^- was detected in solution at the completion of the reaction.

The formation of Cl^- is slower than the disappearance of the 3,4-DCP from the solution. Indeed, in a solution containing $3.0 \times 10^{-4}M$ of 3,4-DCP, $5.0 \times 10^{-5}M$ Fe^{2+}, $5.0 \times 10^{-3}M$ H_2O_2 and $5.0 \times 10^{-3}M$ of $HClO_4$, the dichlorophenol disappears completely in < 25 min of reaction, while the expected stoichiometric amount of free Cl^- ($6.0 \times 10^{-4}M$) in solution for complete degradation of 3,4-DCP is obtained only after 250 min of reaction. This suggests that chloroaliphatic intermediate(s) may be formed after the opening of the benzene ring. This time lag between the disappearance of the phenol and the complete appearance of the product(s) (here, Cl^- ions) depends on the number of chloro substituents on the aromatic ring. For instance, for the mono-chloro derivatives, the disappearance of the chlorophenols and the appearance of stoichiometric amounts of chloride occur at nearly similar times (see Fig.13). The results of Table 4 also indicate that a $HClO_4$ effect exists, and at higher concentrations of this acid the reaction is slower.

The disappearance of 3,4-DCP ($3.0 \times 10^{-4}M$) as a function of time, for three different concentrations of $HClO_4$, is reported in Fig.14; the other reagents were kept at $[Fe^{2+}]$ = = $5.0 \times 10^{-5}M$, $[H_2O_2]$ = $5.0 \times 10^{-3}M$. Thus a tenfold increase of $[HClO_4]$, from $5.0 \times 10^{-3}M$ to $5.0 \times 10^{-2}M$, leads to an increase of $t/2$ from $\sim$ 7 min to $\sim$ 85 min. In the degradation of other chlorophenols, an increase of $[HClO_4]$ increases the induction period for the degradation process. A typical example is portrayed by the decomposition of 4-CP. Where $[HClO_4]$ is $1.5 \times 10^{-2}M$, no detectable degradation occurs for $\sim$ 100 min. The $t/2$ is > 180 min (Table 4).

Another important parameter to consider was the effect of the Fe^{2+} concentration.

Increasing the $[Fe^{2+}]$ in solution for a fixed $[H_2O_2]$ at $5.0 \times 10^{-3}M$ increases the rate of decomposition. At concentration > $2.0 \times 10^{-4}M$ in Fe^{2+}, the decomposition was too fast to follow with our techniques for reasonably reproducible results.

Finally the effect of Fe^{3+} on the degradation of 4-CP in a H_2O_2/chlorophenol mixture was investigated. The reaction was carried out at $10^{-2}M$ in $HClO_4$. Addition of Fe^{3+} (instead of Fe^{2+}) is inconsequential in the degradative process. However, an equivalent concentration of Fe^{2+} brings $t/2$ to $\sim$ 50 min.
Equimolar amounts of Fe^{3+} and Fe^{2+} in the same reaction mixture increase the reaction rate ($t/2 \sim$ 20 min). No doubt, Fe^{3+} is an important species in the complex degradative process.

The results herein reported may be interpreted on the basis of the following considerations. The interaction of iron(II) ions with hydrogen peroxide yields $OH\cdot$ radicals and iron(III)

(equation 14). The OH· formed, can easily

$$Fe^{2+} + H_2O_2 \xrightarrow{\ k = 63\ M^{-1}s^{-1}\ (298K)\ (5)\ } Fe^{3+} + OH· + OH^- \quad (14)$$
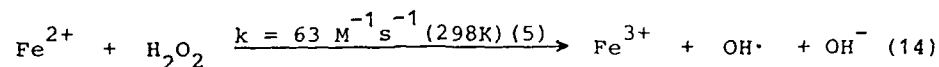
interact with an aromatic compound inasmuch as OH· radicals are good electrophiles.

In the presence of oxygen, oxidation of the intermediate species $(HOCl\overset{\cdot}{C}_6H_3H(OH)$ is preferred even if dimerization is still possible.

By analogy with earlier work on hydroxylations of aromatics, the degradative oxidation of chlorophenols probably proceeds via a hydroxylated species following which ring opening occurs to yield aldehydes and ultimately degradation ensues to CO_2 and Cl^-.
Various factors may contribute to the above experimental observations.

It can be tentatively suggested as a first step the formation of a radical cation by acid-catalyzed dehydration of the radical formed between the interaction of OH· with the chlorophenols (reaction 15). Evidences of the formation of radical-cations in acid media have been reported for methoxylated benzoic

(15)
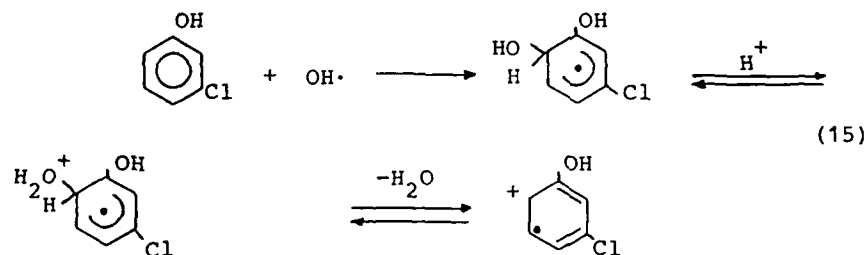
acids. The different stabilities of the radical-cations formed for other chlorophenols may be an important factor responsible for the induction period observed in the degradation of chlorophenolic compounds at higher acidity. In fact, chlorine substituents in ortho and para positions can stabilize the positive charge of the radical-cation of eq. 15 better than meta-chlorine.

An alternative route of degradation is shown in eq. 16:

$$(HO)Cl\overset{\cdot}{C}_6H_3(OH) \xrightarrow[-HCl]{oxidation} HOC_6H_3(OH) \quad (16)$$
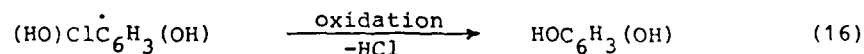
The formation of resorcinol as an intermediate product in the degradation reaction of 3-CP has been detected by HPLC technique.
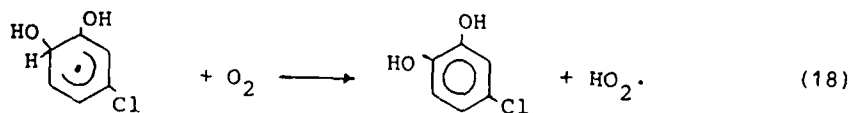
The increase in the oxidation rate of the decomposition of these chlorinated aromatic substrates when the amount of Fe^{2+} is increased from $3.0 \times 10^{-5}M$ to $2.0 \times 10^{-4}M$ is the result of an increase in the concentration of $OH\cdot$ produced according to reaction 14. Under our experimental conditions, it was not possible to investigate the process at higher $/\bar{F}e^{2+}\bar{/}$ as the reaction was too rapid, even at higher $/\bar{H}ClO_4\bar{/}$.
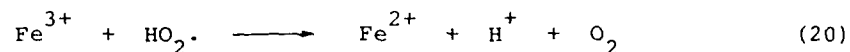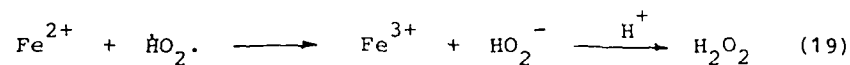
Iron(III) alone with H_2O_2 has very little effect, if any, on the degradation reaction (no $OH\cdot$ radicals can be formed). However, inasmuch as $HO_2\cdot$ radicals form from Fe^{3+}/H_2O_2 mixtures, these are inconsequential in the first step of the decomposition. Equivalent amounts of Fe^{2+} and Fe^{3+} increase the rate of oxidation more than the presence of Fe^{2+} alone. Furthermore, in a typical experiment (cf. Table 4), the amount of Fe^{2+} is catalytic compared to H_2O_2 and chlorophenol concentrations. Since reaction 14 is stoichiometric and almost complete degradations of the chlorophenols are obtained, reduction of Fe^{3+} to Fe^{2+} must occur. These considerations suggest the possible occurrence of reaction 17. That Fe^{2+}/Fe^{3+} mixtures enhance the

$$(17)$$
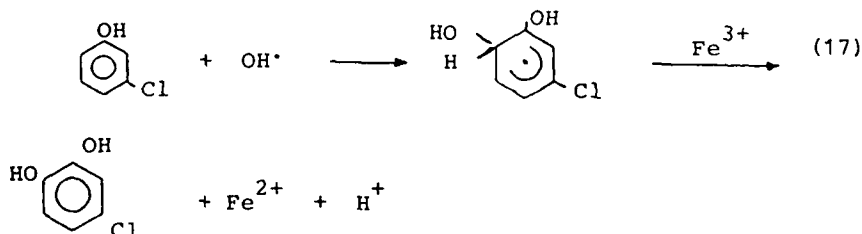
degradation of the chlorophenols, while the presence of a large concentration of $HClO_4$ inhibits the reaction, is indicative of the competitiveness of reactions 15, 16 and 17.

Oxygen also has an effect on the hydroxylation reactions since it can act as a radical scavenger as noted in reaction 18. Following this, the $HO_2\cdot$ species can successively react with either Fe^{2+} or Fe^{3+} (reaction 19,20) to regenerate H_2O_2 and Fe^{2+}.

$$(18)$$

$$Fe^{2+} + \dot{H}O_2 \cdot \longrightarrow Fe^{3+} + HO_2^- \xrightarrow{\;H^+\;} H_2O_2 \quad (19)$$

$$Fe^{3+} + HO_2 \cdot \longrightarrow Fe^{2+} + H^+ + O_2 \quad (20)$$

Further reaction of these hydroxylated aromatic species with the oxidizing agents in solution leads to the degradation products.

The disappearance of chlorophenols and apparance of free chloride in solution (Fig.13) follow neither first nor second order kinetics, which appear to be quite complex. Further studies will address the nature of the various species in the hope of clarifying the pathway(s) of the degradation process.

Comments

These studies have shown that the utilization of Fenton's reagent affords an attractive possibility of decomposing chlorinated aromatic contaminants. Other studies, in program are directed at the potential degradation of pollutants and may contribute to the resolution of environmental problems such as the control and disposal of wastes.

III. CHEMICAL REACTIONS IN MICROEMULSIONS AND MICELLES

Microemulsions are transparent dispersions of an oil in water (O/W) or water in oil (W/O) in the presence of a surfactant and a cosurfactant.
These dispersions form spontaneously upon mixing and contain spherical droplets, having usually diameters of 10-60 nm. The O/W microemulsions have similarities to normal micelles in water, and can be described as a stable collection of "oil" microdroplets in an aqueous continuous phase, while W/O microemulsions should be similar to the reverse micelles in apolar solvents.

The submicroscopic aggregates can bring reactants together or keep them apart, and can also extent a medium effect. As reaction media however the microemulsions can incorporate relatively large amount of solute and the volume of the disperse phase can generally be varied over a fairly wide range.

Whereas reactions in micelles have been studied extensively, processes in microemulsions (particularly electron transfers) have been scarcely examined.

Two model reactions (see below) have been investigated in order to obtain informations on the properties of microemulsions as reaction media.

III.1. Ground State Charge Transfer Complexes in O/W Microemulsions

Solute migration in microheterogeneous media still raises a number of questions as to its rates and mechanism.

In aqueous micellar solution, a number of investigations have led to a reasonable understanding of the solubilization of solutes as well as some of the mechanisms of their migration. For example, a dynamic exchange of CH_2I_2 takes place between bulk and sodium dodecylsulphate $(10^{-1}$ M) micelles at a rate of the order of 10^7 s^{-1}. It is clear however that the rate of such processes is highly dependent upon the hydrophobic/hydrophilic character of the solute, as well as the nature of the microheterogeneous aggregates.

In order to clarity this point the formation of the ground state charge transfer complex between durene and chloranil was investigated in CH_2Cl_2 and in oil-in-water (O/W) microemulsions. The CH_2Cl_2 or CH_2Cl_2/hexadecane microemulsion systems are stabilized by a cationic (hexadecyltrimethylammonium bromide) surfactant and 1-butanol as cosurfactant.

Since the equilibrium constant for the formation of charge transfer complex is 0.66 M^{-1} in CH_2Cl_2 and 8.4 M^{-1} in µE,

it is evident that the compartmentalization introduced by the microemulsion structure favors drastically the CT complex for mation.

If one writes the law of mass action with respect to the non-aqueous volume, one would aspect to have

$$\frac{|DA|_0}{|D|_0 \; |A|_0} = K_H \tag{21}$$

where concentrations are measured with respect to the oil pha se. This may be transformed to use average concentration (with respect to the total volume). One obtains

$$\frac{|DA|}{|D| \; |A|} = K_H \; \frac{V_t}{V_0} = K_M \tag{22}$$

where V_t is the total solution volume and V_0 is the "oil pha-se" volume. From the measured K_H and K_M one obtains that V_t/V_0 should be 12.6.

Under the assumption that there is no change in the densi-ty of water in the microemulsion systems, the ratios V_t/V_0 for the two microemulsions can be evaluated to be ca. 3, which does not account for the experimental ratio K_M/K_H. For the O/W systems considered here, the structure of the droplets may be described as a stable collection of "oil" microdroplets in an aqueous continuous phase. Each droplet consists of a "bulk" oil drop surrounded by a thick interphase consisting mainly of alcohol molecules and cationic surfactant. Then, if the ra tio V_t/V_0 is calculated as $\Sigma(w_i/d_i) \, / \, \Sigma(w_0/d_0)$ (where d is the density, the substript c refers to CH_2Cl_2 and hexadecane and i to all the components) values ranging from 7 to 10 can be estimated (depending on the microemulsion and on the assump tions concerning the density of the non-oil material).
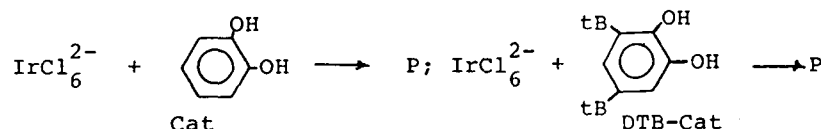
Thus, if the charge transfer complex is confined in CH_2Cl_2 or CH_2Cl_2/hexadecane component, the change in the equilibrium constant from homogeneous to microemulsion medium should main ly be due to the decrease of the available volume for the so-lutes (A and D) in the microemulsion system. In this last hy-pothesis, the apparent lack of effect of the compartmentali-zation should be related to the solute (or complex) dynamic exchange between microemulsion droplets.

Using stopped-flow experiments, attempt was performed to measure the rate at which equilibrium is attained when mix-ing two identical microemulsions, one containing D and the other containing A, or one containing the charge transfer com

plex and the other only the microemulsion. Under all conditions, the expected equilibria were reached faster than the 1 millisecond time response of our equipment. Whatever the mechanisms involved we can say that equilibrium is obtained at a rate faster than 1×10^3 s^{-1}.

III.2. Electron Transfer Reactions in µE

Degradation reactions often go through initial redox steps. As an example of electron transfer reaction involving organic substrates and oxidizing metal complexes in µE systems the following reactions have been selected:

$$IrCl_6^{2-} + \underset{Cat}{\text{(catechol)}}\text{-OH} \longrightarrow P; \quad IrCl_6^{2-} + \underset{DTB\text{-}Cat}{\text{(di-tert-butylcatechol)}}\text{-OH} \longrightarrow P$$

- Pseudoternary phase diagram
The single-phase limits were experimentally determined (Fig. 15). By comparison with other phase diagrams reported for the same Butanol/SDS ratio, and from conductivity measurements (Fig. 16), it can be assumed that the microstructure changes from swollen micelles, through a bicontinuous phase, to reverse micelles. Whereas the lower phase limits can be explained by various current theories, the upper limit can be rationalized in terms of a failure of the bulk aqueous phase.
The kinetic measurements were performed along the dilution lines, in which the Butanol/SDS/Toluene ratio was kept constant (see Fig. 15).

- Kinetic measurements
The variation of k_{exp} measured by stopped-flow as a function of the microemulsion composition is depicted in Fig. 17. For both investigated catechols, the following behavior has to be noted: - at higher water fractions inhibition is observed (which is more pronounced for DTB-Cat); - at lower water content there is an increase in reaction rates inversely dependent on the oil content.

- Three pseudophases model
A simple microemulsion model, consisting of three distinct pseudophases, without any assumptions about the microstructure, is proposed.
The following kinetic equation holds:

$$k_{exp}\,c_{\mu E} = \chi_w \bar{v}_w k_w \frac{\overline{c}_{A(w)}\,\overline{c}_{B(w)}}{c_{A(TOT)}\,c_{B(TOT)}} + \chi_I \bar{v}_I\, k_I \frac{\overline{c}_{A(I)}\,\overline{c}_{B(I)}}{c_{A(TOT)}\,c_{B(IOT)}} + \chi_o \bar{v}_o\, k_o \frac{\overline{c}_{A(o)}\,\overline{c}_{B(o)}}{c_{A(TOT)}\,c_{B(TOT)}} \quad (23)$$

where: k_{exp} is the second order rate constant in the micro-emulsion; δ's are the densities of the microemulsion and of pseudophases; k's are the specific rates constants in each phase; C's are the local concentrations of the reagents expressed in moles/mass; x's are the pseudophases molar fractions.

The partition coefficients for each reagent R (A=IrCl$_6^{2-}$, B = = catechols), are defined as follows: P_{WI}^A, P_{WI}^B, P_{WO}^A, P_{WO}^B, where:

$$P_{WF}^R = EXP\left(\frac{\mu_W^{OR} - \mu_F^{OR}}{RT}\right) = \frac{\chi_F^R \gamma_F^R}{\chi_W^R \gamma_W^R}$$

By substituting into equation (23):

$$k_{EXP} = \frac{\frac{k'_W}{\chi_W} + \frac{k'_I}{\chi_I} P_{WI}^{'A} P_{WI}^{'B} R_I^2 + \frac{k'_O}{\chi_O} P_{WO}^{'A} P_{WO}^{'B} R_O^2}{\left(1 + P_{WI}^{'A} R_I + P_{WO}^{'A} R_O\right)\left(1 + P_{WI}^{'B} R_I + P_{WO}^{'B} R_O\right)} \qquad (24)$$

where $k'=k.\delta$, $P_{WF}^{'R} = P_{WF}^R \cdot \gamma_W^R/\gamma_F^R$, $R_I = (\Sigma_i\ n_i)_I / (\Sigma_i\ n_i)_W$; $R_O = (\Sigma_i\ n_i)_O / (\Sigma_i\ n_i)_W$.

In order to solve the equation (24), it is necessary to calculate the terms R_I and R_O.

Some assumptions about the composition of each pseudophase must be made:

$$(\Sigma_i\ n_i)_W = n_{W(W)} + n_{But(W)} \qquad (25)$$

$$(\Sigma_i\ n_i)_I = n_{W(I)} + n_{But(I)} + n_{SDS(I)} + n_{Tol(I)} \qquad (25)$$

$$(\Sigma_i\ n_i)_O = n_{But(O)} + n_{Tol(O)}$$

Thermodynamics imposes that the components present in each pseudophase must be in equilibrium. The eq. (24) and the appropriate mass balances can be solved in terms of mass transfer constants and activity coefficients. Since the system is far from ideality, another approach which takes in account the mutual solubility limits between the components, can be also proposed.

The moles of the components in each pseudophase can be related through proportionality constants α. It is assumed, in other words, that each pseudophase is always saturated with respect to the components present in defect. α's coefficients are in fact solvation numbers.

$$n_{But(W)} = \alpha_1\ n_{W(W)}\ ;\ n_{W(I)} = \alpha_2\ n_{SDS(I)} + \alpha_3\ n_{BUT(I)}$$

$$n_{But(O)} = \alpha_4\ n_{Tol(W)}\ ;\ n_{Tol(I)} = \alpha_5\ n_{SDS(I)} \qquad (26)$$

where α_1 represents the solubility of n–Butanol in water (0.017); α_2 is the hydration number for SDS in the interphase; α_3 is the solubility of water in n–Butanol (ca.1); α_4 is the solubility of n–Butanol in Toluene (   ); α_5 represents the average number of Toluene molecules per surfactant. It is obvious from these assumptions that the present model is not valid at the corners of the phase diagram.

- Analysis of the experimental data
The multiparametric kinetic equation was solved by computer simulation using eq. (24), (25), (26) with the following assumptions:

a) partition of microemulsion components. Since the solubilities of Butanol in water and Toluene are very low, $\alpha_1 = \alpha_4 = 0$. α_2 and α_3 are fitted by assuming that the upper demixing line is due to the failure of the aqueous pseudophase. The best fitting curves   gave the following values: $\alpha_1 = \alpha_4 = 0$, $\alpha_2 = 3-3.5$, $\alpha_3 = 1$, and $\alpha_5 = 1$. The hydration number for SDS (α_2) is in agreement with the literature data.

b) partition of reagents. $P_{WF}^{/R}$ is assumed to be constant. The estimated $P_{WF}^{/R}$ values for catechols have to be consistent with the partition data obtained both from kinetic and HPLC measurements for SDS, whereas $P_{WF}^{/\,IrCl_6^{2-}}$ must be very low.

c) kinetic parameters. k_W was measured as a function of dissolved Butanol. We used in the fitting the k_W value obtained in Butanol-saturated solution. k_I is a fitting parameter ($k_{But} \leq k_I \leq k_W$. k_{But} is the specific rate in the water-saturated Butanol solution). In eq. (24) the term depending on k_O was neglected.

On the basis of the above mentioned assumptions, the fitting parameters to be evaluated are: P_{WI}^B, P_{WD}^B, P_{WI}^A, k_I.

The obtained fitting curves are shown in Fig. 17.
They were calculated using the following values:

	k_W(exp)	k_I	$P_{WI}^{/\,IrCl_6^{2-}}$	$P_{WI}^{/Cat}$	$P_{WO}^{/Cat}$
Cat	$3.9\ 10^3$	$7.5\ 10^3$	0.2	25	35
DTB-Cat	$7.0\ 10^4$	$3.2\ 10^4$	0.2	$5.0\ 10^4$	$5.0\ 10^5$

where $P_{WF}^{/R} = 55.5(K_B^R + \bar{v}_r)$; $\bar{v}_r$ is the molar volume of the interphase; K_B^R is the usual binding constant (M^{-1}).

The previous hypotheses have been further tested by investigating an electron transfer reaction between two polycharged anions in the same microemulsion medium (i.e. SDS/1-butanol/toluene/water-0.09 M NaCl - 0.01 M HCl). The test reaction was the electron transfer reaction between hexachloroiridate(III) and 12-tungstocobaltate(III). The charge of the surfactant and the charge and the low hydrophobicity of the reagents ensure that the reaction would take place in the water pseudophase, and thus that the reaction rates would be sensitive to the 'effective volume' of the aqueous region. The reactants play the role of local probes in microemulsion medium and thus it will be possible to infer also some remarks about the structure of the micro-emulsion in the surfactant- or in the oil-rich region.

The experimental rate constants as function of the microemulsion composition are reported in Fig. 18, where the dilution lines correspond to a fixed ratio between SDS/1-butanol/toluene. It can be noted that at low water content there is an increase in the reaction rates, with respect to the aqueous solution, which is dependent on the oil content. For dilution lines with high oil content the rate diverges asimptotically when the upper demixing line ia approached. In absence of oil (line 0) the increase is quite low and it is comparable with the increment due to the ionic strenght. The rate constants measured along dilution lines 1 and 2 have a behavior intermediate between line 0 and lines 3,4,5.

The equation previously proposed is not able to predict the observed kinetic behavior for all microemulsion compositions if α values are taken constants. The fitting curves are shown in Fig. 18 as dashed lines. The valu of P for $IrCl_6^{3-}$ of 0.15 was taken comparable with that of $IrCl_6^{2-}$ evaluated previously, while the partition coefficient of the 12-tungstocaobaltate(III) is found slightly less, 0.02,. This value is consistent with the anion charge and its very low hydrophobicity. The simultaneous fitting of the upper demixing line and of the kinetic data on dilution lines 3,4,5 require that the degree of dissociation of the surfactant will be quite high, i.e. α =0.55, but still reasonable if almost all the alcohol lies in the surfactant palisade of the interface. In fact thevalue of   for micelles increases when alcohol is added.

COMMENTS

The proposed three pseudophase model is able to predict quantitatively the rate of reaction in microemulsion, in regions of the phase diagram where the solution is structured. The partition coefficients for reagents, the hydration number of the surfactant, and also the mean degree of dissociation agree quite well with reported or estimated values obtained using other techniques.

The comparison between kinetic data for a proper reaction and the prediction of the model, makes a clear distinction between microemulsion compositions which lead to a structured and a non-structured systems and allows to obtain some information on the hydration of the surfactant and of the cosurfactant without assuming any microscopical geometrical configuration of the solution.

The microemulsion systems appear suitable media for carrying out redox reactions involving highly hydrophobic compounds and hydrophilic metal complexes.

The kinetics and mechanism of reactions in O/W microemulsions have been extensively reviewed (ref. 14).

III.3 Electron Transfer Reactions in Micelles

A general phenomenological approach based on
(i) the two pseudophase approximation
(ii) a proper definition of the transfer constants between
the pseudophases in term of molar fractions
(iii) an explicit hypothesis that relates the number of bound
molecules or ions to the surfactant concentration
(iv) a semiempirical calculation of the activity coefficients
of bound charged species at the micellar surface

permits the prediction of the reactivity as a function of
micelle and added salt concentrations.

Kinetic experiments were designed to test the model;
the ivestigeated system was the electron transfer reaction
between hexachloroiridate(IV)-Iron(II) in the presence of
hexadecyltrimethylammonium chloride or sulfate with added
sodium chloride or sulfate.

The fit with the model is shown in Fig. 19.

The dissociation degree of the micelle is found comparable
with literature values.

III.4 Interactions of Solutes with Micelles

The partition equilibria of a series of thirty substituted phenols bearing different chemical groups between aqueous solutions and sodium dodecylsulfate micelles has been investigated by using micellar high-performance liquid chromatography and by studying the variation of the acidity constant.

The contribution of each substituent to the free energy of transfer from water to micelles has been estimated. Values are listed in Table 5 and 6.

The group contribution approach is shown to be valid for polysubstituted compounds under well defined conditions, as shown in Fig. 20.

A comparison with partition coefficients obtained in classical two-phase system (1-octanol/water)is discussed.

IV. CHARACTERIZATION AND PROPERTIES OF FUNCTIONALIZED SUR-FACTANTS

Functionalized surfactants are amphiphilic molecules in which the polar head group can exhibit a chemical reactivities, such ad complexing capability or electron transfer properties.

The complexing behavior could be used in chemical separations and in catalytic processes in organized assemblies.

As model system, the properties of a series of compounds containing the same chelating moiety, namely 4-aminosalicylic acid, with different alkyl chains, was investigated. The structure of the ligands (PAS-C_n) is the following:

$$R-CONH-\langle\bigcirc\rangle-COOH \qquad C_n: C_{n-1}H_{2n-1}-CO$$
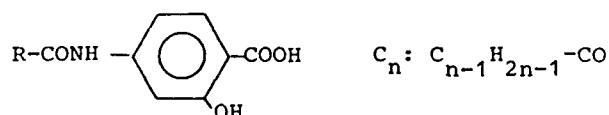
Since aggregation occurs for these compounds only at high pH values, a study of complexing properties of aggregates in the presence of usual transition metal ions cannot be performed. At lower pH, however, the PAS-C_n molecules can be readily solubilized in the presence of nonionic surfactants (e.g. Brij 35: polyoxyethylene(23)dodecanol) and the obtained mixed micelles exhibit complexing capability in acidic media.

- Binding Constants of Ligands with Nonionic Micelles
The acid-base properties of the amphiphilic ligands change in the presence of micellar aggregates due to the well known partition equilibrium of both the acid and anionic form. A continuous increase in the apparent pK_a was observed with increasing concentration of micellized surfactant.

According to the simple pseudophase model of Berezin, the binding constants between the ligands and the micelles have been calculated using the following equation:

$$K_{a(app)}^{-1} = K_{a(w)}^{-1} + K_{HA} \cdot K_{a(w)}^{-1} \cdot C_D \qquad (27)$$

where $K_{a(app)}$ is the dissociation constant of carboxylate group in the presence of Brij 35, $K_{a(w)}$ is the same constant in water, K_{HA} is the binding constant of the undissociated PAS-C_n to the micelles and C_D is the concentration of micellized surfactant ($C_D = C_{tot} - CMC$).
The critical micellar concentration for Brij 35, measured with the surface tension method is 6×10^{-5} M, in the experimental conditions.

For the investigated PAS-C_n ligands, the binding constant

for the undissociated form clearly increases with n_1 from
170 M^{-1} for C_2 and 500 M^{-1} for C_4 up to ca. 1500 M^{-1} for C_7,
whereas for the anionic form it becomes significant only
for C_7 (110 M^{-1}). The obtained data is in good agreement
with the values estimated from $pK_{a(app)}$ shift, at low surfac-
tant concentration, and allow us to define a minimum chain
length for the ligand in order to have a strong binding to
the micelles, both in acidic or anionic form.

- Complex Formation Constant in the Presence of Micelles
The kinetics and the complex formation equilibria in the pre
sence of nonionic micelles have been also investigated, at
constant acidity. The stoichiometry was assessed by using
Job's method and the apparent stability constants were eva-
luated according to Frank and Ostwalt procedure, as previou
sly reported for the system iron/salicylate in homogeneous
aqueous solution.
    For the equilibrium reaction:

$$Fe^{3+} + HSal^- \longrightarrow Fe\ Sal^+ + H^+$$
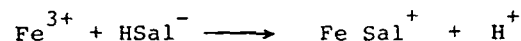
where $HSal^-$ indicates the dissociated chelating moiety of
the ligand, the observed changes in the apparent formation
constants (K_c) can be directly related with the variation
of the apparent pK_a, previously discussed. In the conditions
reported in the experimental section, the K_c values lie in
the range $(2.5-4.0) \times 10^3$.
    The experiments performed clearly showed that, whereas
the complexation of iron(III) is not very much dependent on
the ligand hydrophobicity, the association of the charged 1:1
chelates to the micelles and then the efficiency of the con
centration process, markedly increases.

- Extraction of Iron(III) from Micellar Solutions
The surfactant system Triton X 100 / BL 4.2 was chosen becau
se its suitable cloud temperature range and the good solubi-
lizing capability towards the ligands.
    The analyte content, after extraction, was determined both
in the micellar and in the aqueous rich phase by VIS-spectro
photometry. Calibration curves were made with micellar pha-
ses containing the dissolved ligands, in the absence of iron
(III). To these solutions, separated by centrifugation, were
added known amounts of analyte and the absorbances were re-
corded.
    The standard addition method was also applied to the ex-
tracted micellar layers containing iron(III). The results ob
tained with both procedures were in good agreement, as well
as which obtained from DC-plasma spectrometry after analysis

of the aqueous dilute phases.

The extraction efficiency was then calculated from at least four independent measurements; the influence of the experimental parameters was also investigated.

Fig. 2.1 shows the effect of the ligand hydrophobicity on the analyte recovery, measured at pH 3.5, in the presence of Triton X-100 (1% w/v) and BL 4,2 (1% w/v); added $NaNO_3$: 5% w/v; iron(III): 1×10^{-4} M and PAS-C: 2×10^{-3} M.

As it can be seen, quantitative recovery of iron(III) has been obtained in the reported conditions using the more hydrophobic compounds (PAS-C_{10} or higher analogues). However, the lower solubility of these long chain molecules can limit the ligand concentration available in the system, keeping the volume of extraction micellar phase constant.

The extraction performances under different experimental conditions (i.e. varying the pH, the composition of surfactant mixtures, the amount of chelating compound) were also investigated for our test system. The results are shown in Table 7.

- Kinetics of Complex Formation in Micellar Media

The kinetics for complexation reactions of Iron(III) with the PAS-C_n ligands (n= 2 and 4) was studied by stopped-flow technique in aqueous acidic solutions containing varying amounts of the non ionic micelle forming surfactant Brij-35.

The kinetic findings indicate that the complexation reactions occur in the aqueous intermicellar phase and that the reactions of the $FeOH^{2+}$ ion with both the neutral and monoanionic forms of the ligands contribute significantly to the overall complex formation rate, a dissociative ion-pair mechanism being operative. The reaction scheme is depicted in Fig. 22.

The resulting kinetic expression is

$$\frac{1}{k_f} = \frac{K_{a,w} + [H^+]}{k_{f,w} K_{a,w}} + \frac{(K_{a,w} K_L' + K_L [H^+]) C}{k_{f,w} K_{a,w}}$$

and the experimental data plotted accordingly are reported in Fig. 23 and 24.

The binding constants of the iron(III) monocomplexes and the neutral ligands to the nonionic micelles were estimated from the equilibrium and kinetic data, respectively, and collected in Table 8.

- Comments

   The results obtained with the reported amphiphilic
ligands in the extraction process showed that the separation
of charged species is possible, provided a suitable ligand
hydrophobicity. Further developments of these multiphase
extraction systems will require an accurate investigation
of the equilibriaand kinetic processes occurring at the
interfaces, as well as the study of the micellar structure
and properties of the host aggregates.

   Other functionalized surfactants having various complexing
groups and modular lipophilic chains, together with different
nonionic solubilizing surfactants, are presently under
investigation.

   The general features have been reported in an exaustive
review (ref. 19).

Table 1.- Half-lives for the Total Photodegradation of Contaminants Assisted by TiO_2 on Exposure to simulated Sunlight[a].
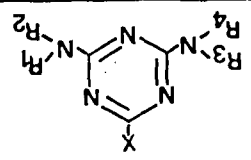
COMPOUND	ABBREV.	CONCENTRATION (ppm)	pH	$t_{1/2}$ (min)
4-chlorophenol[b]	4-CP	6	3.0	14
3,4-dichlorophenol	3,4-DCP	18	3.0	45
2,4,5-trichlorophenol	2,4,5-TCP	20	3.0	55
Pentachlorophenol[b]	PCP	12	3.0	20
Sodium pentachlorophenate	NaPCP	12	10.5	15
Chlorobenzene	CB	45	2.5	90
1,2,4-trichlorobenzene	1,2,4-TCB	10	3.0	24
2,4,5-trichlorophenoxyacetic acid	2,4,5-T	32	3.0	40
4,4'-dichlorodiphenyltrichloro-ethane[c]	4,4'-DDT	1	3.0	46
3,3'-dichlorobiphenyl[c]	3,3'-DCB	1	3.0	10
2,7-dichlorodibenzo-p-dioxin[c]	2,7-DCDD	0.2	3.0	46

a: Concentration of catalyst, 2.0 g/l; aerated aqueous solutions; wavelength >330 nm.

b: Wavelength >310 nm.

c: Adsorbed on TiO_2

TABLE 2

Formula generale	Nome Chimico	Nome Comune	X	R_1	R_2	R_3	R_4
	2-cloro-4-etilammino-6-iso-propilammino-1,3,5-s-triazi-na	ATRAZINA	Cl	H	C_2H_5	H	$CH(CH_3)_2$
	2,4-disopropilammino-6-me-tossi-1,3,5-s-triazina	PROMETONE	OCH_3	H	$CH(CH_3)_2$	H	$CH(CH_3)_2$
	2,4-diisopropilammino-6-me-tiltio-1,3,5-s-triazina	PROMETRINE	SCH_3	H	$CH(CH_3)_2$	H	$CH(CH_3)_2$
	2-cloro-4-dietilammino-6--etilammino-1,3,5-s-triazi-na	TRIETAZINA	Cl	H	C_2H_5	C_2H_5	C_2H_5

- Erbicidi s-triazinici studiati.

	Ref.	Notes
Direct Photolysis	4	High energy photons; cloroorganic compounds; residues; cyclization compounds.
Indirect Photolysis	5, 122	Solar light; Sensitized required (stability problems); non complete degradation.
Ozone/hv	119	Ozone generator; Ozone storage difficulty; UV lamp required; effective degradation obtained.
H_2O_2/hv	120	Chemical reactant; UV lamp H_2O_2 required; easy to mix; H_2O_2 can not be stored; effective degradation obtained.
Photocatalysis	this work	Heterogeneous system; Solar radiation or UV lamp required; complete mineralization; stable catalyst; no chemical reactant required; applicable to waste water and to drinking water.

TABLE 3

Comparison of degradation methods involving light.

TABLE 4 - Half-lives (t/2; see text) of Decomposition
of Various Chlorinated Phenols: $[Fe^{2+}]$ =
$5.0 \times 10^{-5}M$, $[H_2O_2] = 5.0 \times 10^{-3}M$,
[chlorophenols] = $3.0 \times 10^{-4}M$.

Compound	t/2 at $5.0 \times 10^{-3}M$ HClO$_4$ (min)	t/2 at $1.5 \times 10^{-2}M$ HClO$_4$ (min)
3-chlorophenol	6.5	34
2-chlorophenol	14.5	125
4-chlorophenol	12.5	> 180
3,4-dichlorophenol	6.3	16
2,4,5-trichlorophenol	12	36

TABLE 5

Binding of substituted phenols to SDS micelles and standard energies of transfer per molecule and per group

No.	Compound	$K_n(M^{-1})$	$\Delta\mu_t^0$ (kJ mol^{-1})		Log $P_{o/w}$[a]
			Molecule	Group	
1	Phenol	10[b]	−15.66	–	1.46
2	4-Methoxy	15[c]	−16.65	−0.99	1.34
3	4-Ethoxy-	27.5[c]	−18.16	−2.50	1.81
4	4-n-Butoxy-	108[c]	−21.56	−5.90	–
				−1.67[d]	–
5	4-Phenoxy-	210[c]	−23.21	−7.55	–
6	4-Phenyl-	370[b]-360[c]	−24.58	−8.92	–
7	4-Formyl-	12.5[c]	−16.21	−0.55	1.70[f]
8	4-Acetyl-	21[c]-20[c]	−17.44	−1.78	–
9	4-Propanoyl-	48[c]-44[c]	−19.44	−3.78	–
				−1.63[d]	–
10	4-Carboxymethyl-	36[c]-38[c]	−18.90	−3.24	1.96
11	4-Carboxyethyl-	70[c]-68[c]	−20.45	−4.79	2.47
12	4-Carboxypropyl-	169[c]	−22.67	−7.01	3.04
				−1.88[d]	–
13	4-Cyano-	16[c]-14[c]	−16.67	−1.01	1.60
14	4-Cyanomethyl-	36[c]	−18.84	−3.18	–
15	4-Nitro-	17[c]-15[c]	−16.83	−1.17	1.91
16	2-Carboxamido-	6[c]	−14.40	1.26	1.28
17	2-Acetamido-	8[c]	−15.11	0.55	–
18	4-Methylthio-	49[c]-46[c]	−19.52	−3.86	–
19	3-Trifluoromethyl-	130[c]	−22.02	−6.36	2.95
20	2-N-Phenylcarboxamido-	250[c]	−23.64	−7.98	3.27
21	2-Nitro-4-chloro	44[c]	−19.33	–	–
22	3-Nitro-4-methyl-	42[c]-37[c]	−19.07	–	–
23	2-Chloro-4-bromo-6-Methyl	330[c]	−24.33	–	–
24	4-Nitro-2,6-diodo-	2100[c]	−28.92	–	–
25	3,5-Dimethoxy-	24[c]	−17.83	–	–
26	2,6-Dimethoxy-4-acetyl-	36[c]	−18.84	–	–
27	2-Acetamido-4,6-dichloro-5-methyl-	120[c]	−21.82	–	–
28	1-Naphthol	180[b]	−22.83	–	2.98
29	2-N-Butylcarboxamido-	2100[c]	−28.92	−6.09	–
30	2-N-Phenylcarboxamido	3800[c]	−30.39	−7.56	–

TABLE 6

Standard free energy change for different substituent groups on phenols in various two-phase media

Substituent	$\Delta\mu_t^0$ (kJ mol^{-1})		
	SDS	1-Octanol/water	Hydrocarbon/water
Aliphatic -C- (on phenols)	−2.13	−2.63	−3.16[a]
Aliphatic -C- (on alkanes)	−3.22	−	−3.68[b]
Aliphatic -C- (on arenes)	−2.64	−2.82	−3.35[b]
4-Hydroxy	2.60[c]	4.97	
Hydroxy (on arenes)	1.72	3.81	17.99[b]
4-Cyano	−1.01	−0.80	5.25[a], 7.19[d]
4-Nitro	−1.17	−2.56	
4-Phenyl	−8.92		−9.53[a]
4-Fluoro	−1.38[e]	−1.77	−0.95/−1.37[f]
4-Chloro	−2.68[e]	−5.30	−3.59[a]
4-Bromo	−4.31[e]	−6.45	−4.51[a]
4-Iodo	−6.28[e]	−8.27	−5.02[f]/−6.22[a]
4-Thio-(R)	−1.72	−2.05[g]	
3-Trifluoromethyl	−6.36	−8.50	
2-Carboxamido	1.26	1.03	
2-N-Phenylcarboxamido	−7.98	−10.33	
4-Formyl	−0.55	−1.37/−1.99[h]	
4-O-(R)	0.67	3.34	5.59[a]
4-CO-(R)	−0.42	3.25	
4-COO-(R)	−1.26	0.29	

Table 7. — Extraction Efficiency as a Function of Experimental Parameters for Iron(III)-PAS-C_7

pH	%E	PAS-C_7, M	%E	Triton X100/ BL 4.2, % w/v	%E
2.00	39.0	5×10^{-4}	80.0	0.50:0.50	77.6
2.65	74.5	1×10^{-3}	87.5	0.75:0.75	93.6
3.10	88.4	1.5×10^{-3}	92.0	1.00:1.00	93.7
3.50	93.7	2×10^{-3}	93.7	1.50:1.50	94.0
3.75	94.3				

TABLE 8 : Rate constants[a] for formation and dissociation of iron(III) monocomplexes with PAS-C_2 and PAS-C_4

	PAS-C_2	PAS-C_4
$10^{-3}(k_2 + k_3 K_{OH,w} / K_{a,w})$, $dm^3\ mol^{-1}s^{-1}$	12.9 ± 0.4	8.2 ± 0.3
$10^{-3} k_3$ [b], $dm^3\ mol^{-1}\ s^{-1}$	4.4 ± 0.1	3.6 ± 0.1
$10^{-2} k_4 K_{OH,w}$, s^{-1}	2.2 ± 0.1	2.2 ± 0.1
$10^{-4} k_4$, $dm^3\ mol^{-1}\ s^{-1}$	8.0 ± 0.4	8.0 ± 0.4
k_{-3}, $dm^3\ mol^{-1}\ s^{-1}$	2.3 ± 0.5	1.9 ± 0.1
$10^2 k_{-4}$, s^{-1}	5 ± 4	4 ± 1

[a] $t = 25°C$; $\mu = 0.10\ mol\ dm^{-3}$. [b] With the assumption that $k_2 \ll k_3 K_{OH,w}/K_{a,w}$ (see text).
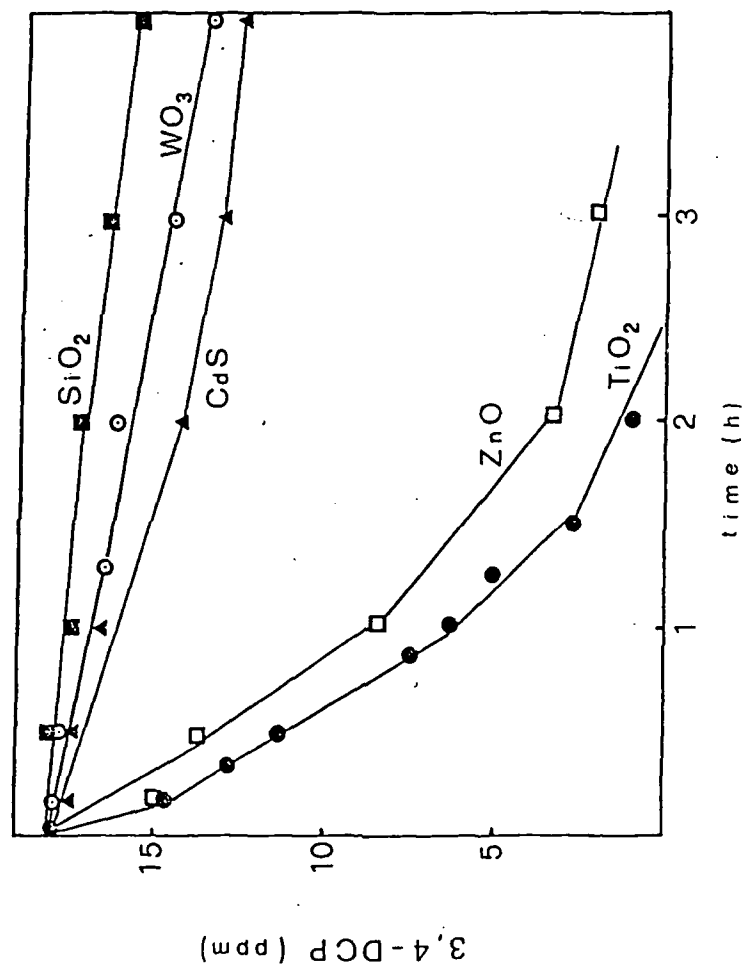
Figure 1. Photodegradation of 3,4-dichlorophenol in the
presence of various semiconductor dispersions;
wavelength of irradiation > 330 nm; initial
3,4-DCP concentration 18 ppm; O_2 present; initial
pH 3.0; unbuffered aqueous solutions; concentration
of catalyst, 2.0 g/l.
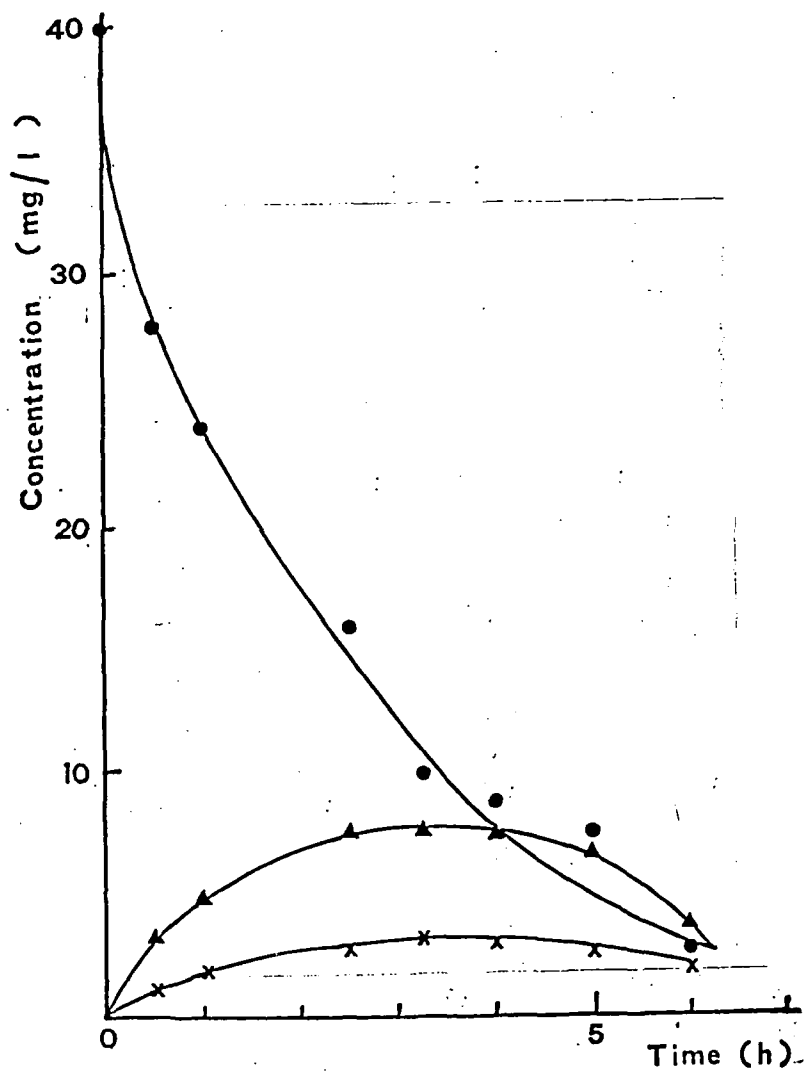
Figure 2   Results of phenol degradation and interme-
diate formation in the presence of TiO_2
(2 g/l); phenol concentration 40 mg/l;
Xenon lamp power 150 W;
(●) phenol; (✗) quinol; (▲) catechol
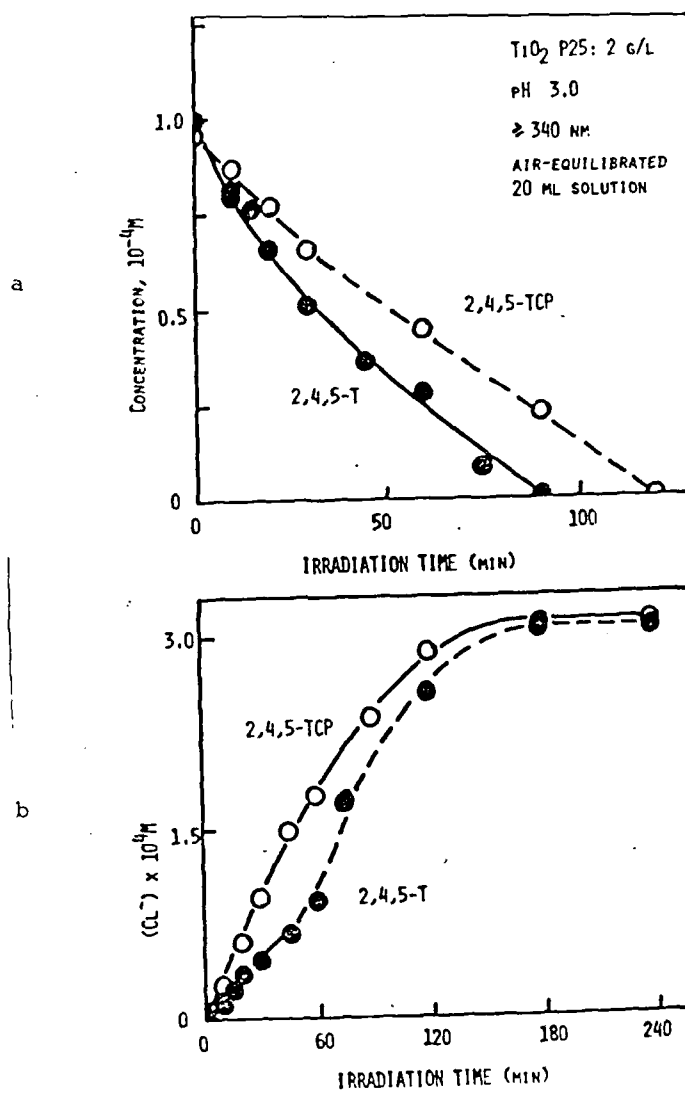
Figure 3 (a) Plot showing the relative decomposition
              of 2,4,5-T and 2,4,5-TCP as a function
              of irradiation time
          (b) Plot showing the formation of stoichio-
              metric quantities of chloride ions as
              a function of irradiation time
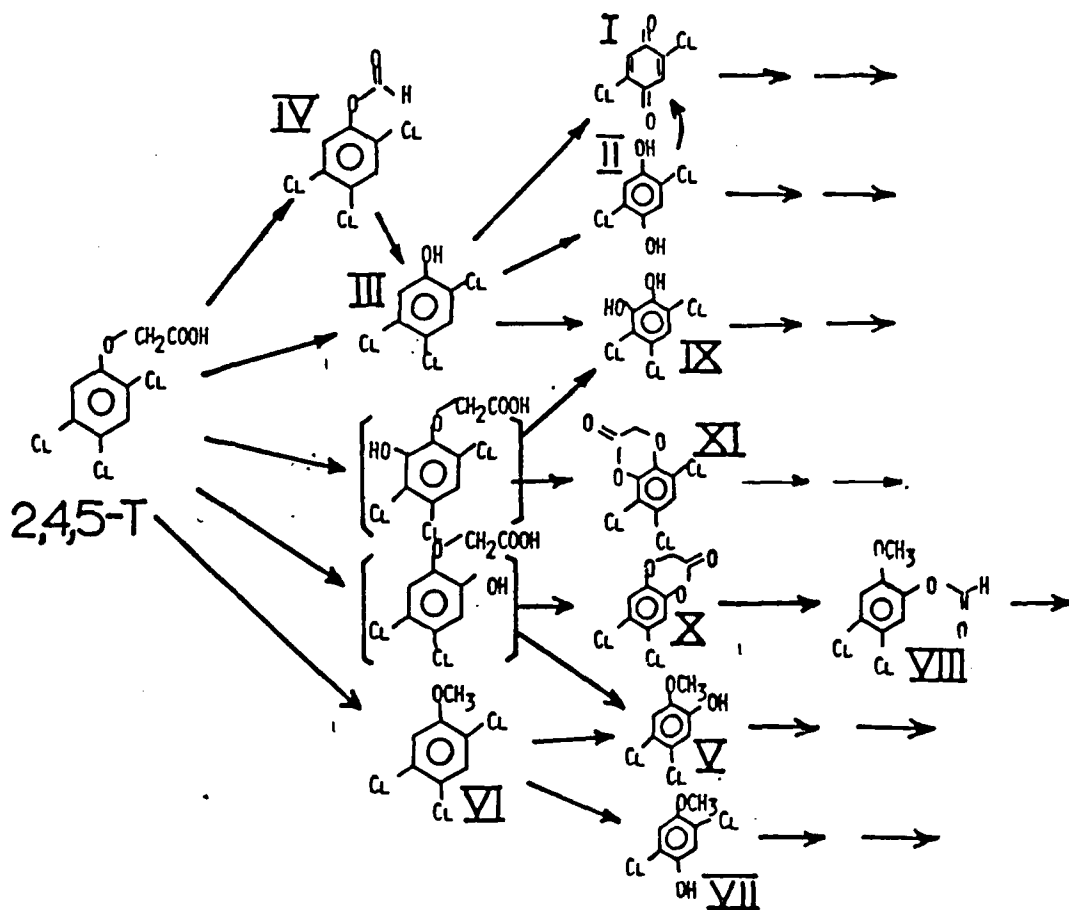
Figure 4   Plausible photodegradation pathway of 2,4,5-T in
the presence of TiO_2 under simulated sunlight
irradiation conditions.
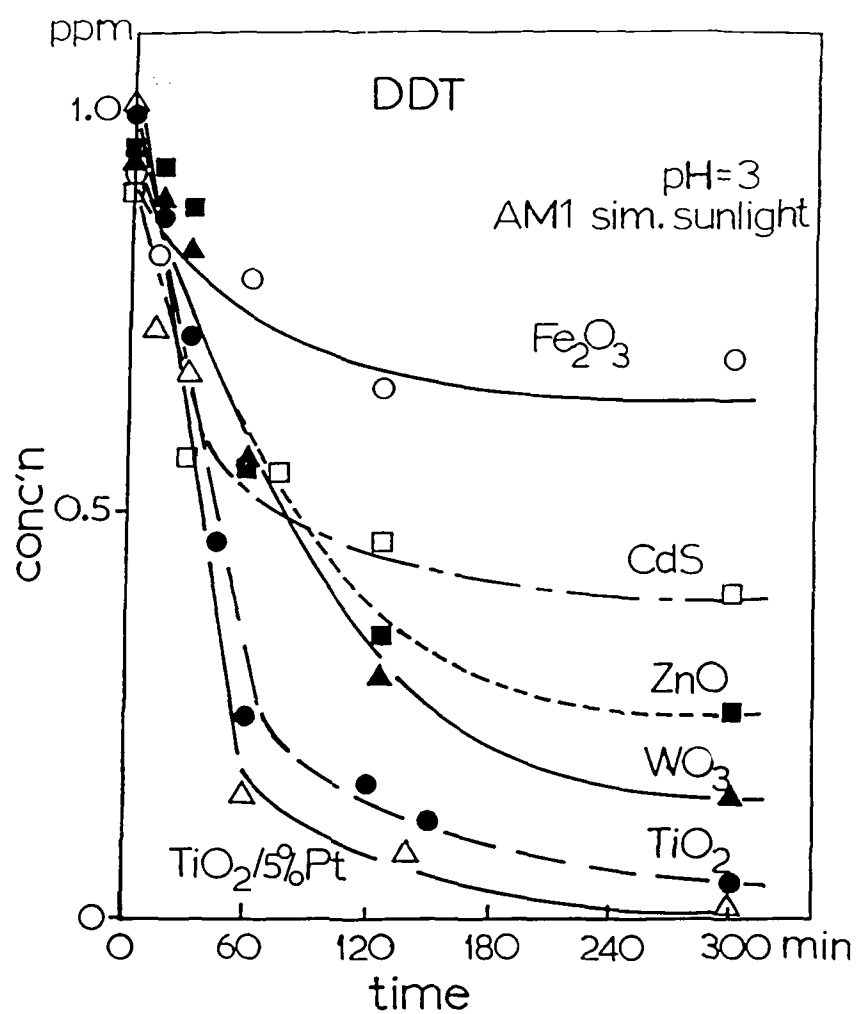
Fig 5 . Plots illustrating the photodegradation of DDT at pH 3 as a function of irradiation time for several semiconductor particulates.
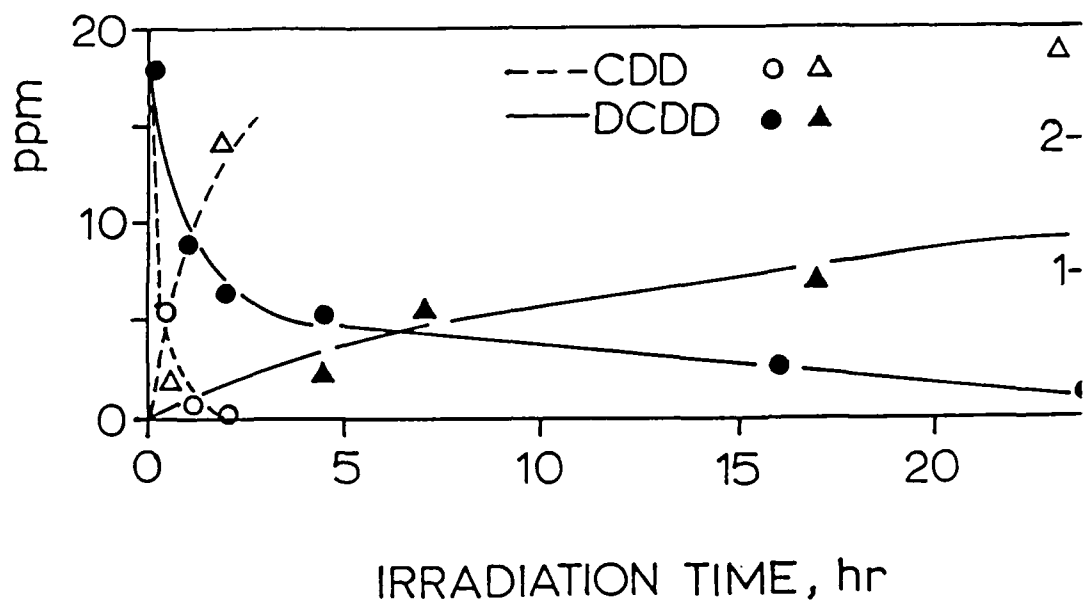
Figure 6 - Concentration <u>versus</u> irradiation time plots in the photodegradation of 2-CDD and 2,7-DCDD; pH 3; TiO_2 = 4 g/L.
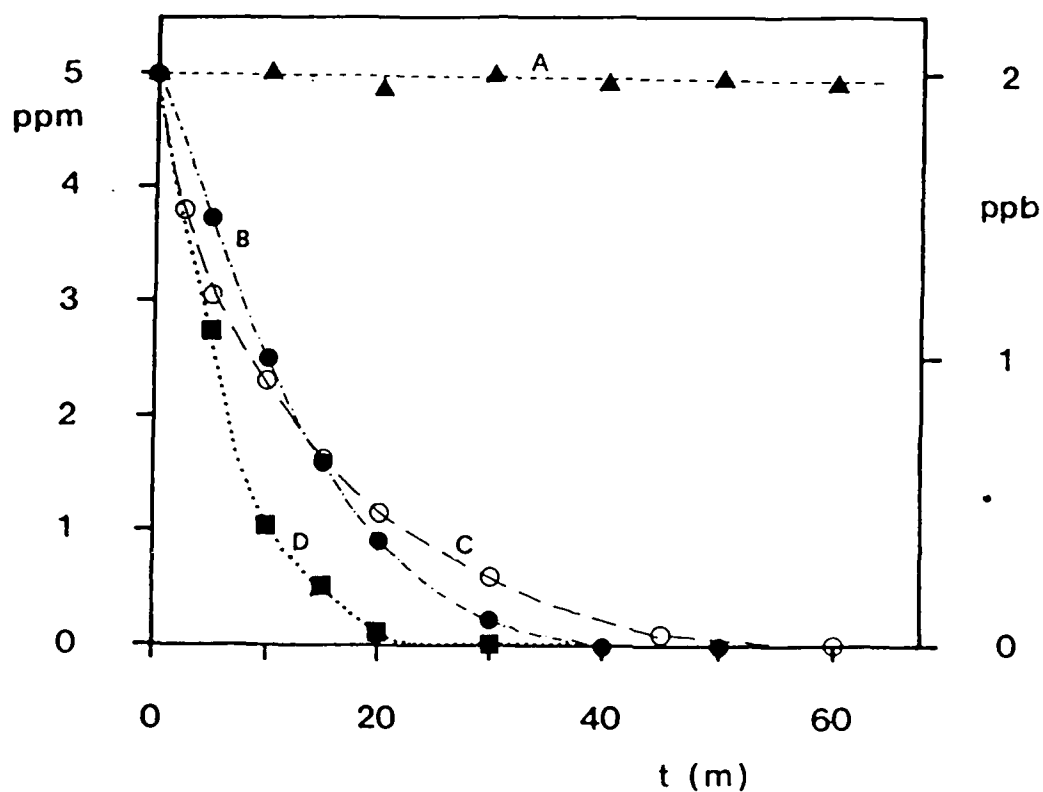
Fig. 7 Plots illustrating the photodegradation of atrazine as a function of irradiation time (Solarbox, $\lambda \geq 340$ nm; unless differently stated): curve A (left scale) : no TiO_2 present - curve B (left scale): 0.1 g/l TiO_2 - curve C (left scale) : 0.1 g/l TiO_2; solar exposure (Turin, May 13, 1987, 4-6 p.m.) - curve D (right scale) : 0.1 g/l TiO_2
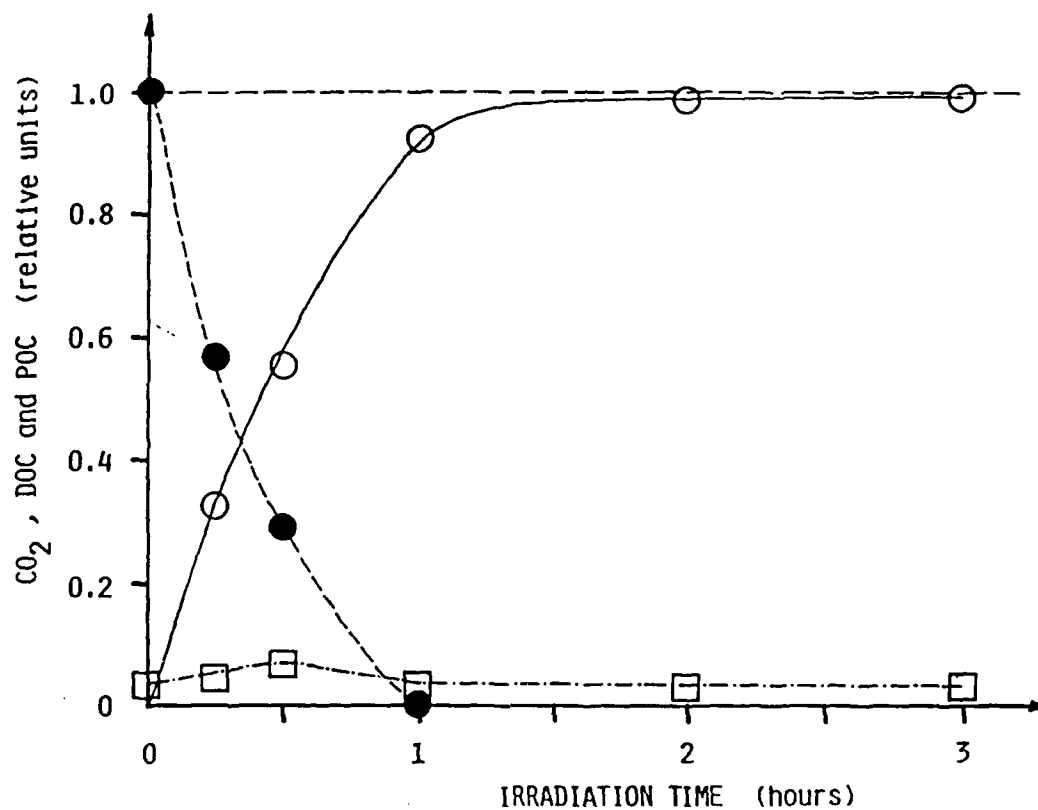
Fig 8

CO_2 ($\bigcirc$) evolution, DOC ($\bullet$) and POC ($\square$) variation as a function of irradiation time for EE. Units are relative to the stoichiometric value: for CO_2, expected from eq.1; for DOC and POC, relative to total carbon. EE initial concentration 100 ppm; TiO_2 2 gL^{-1}.
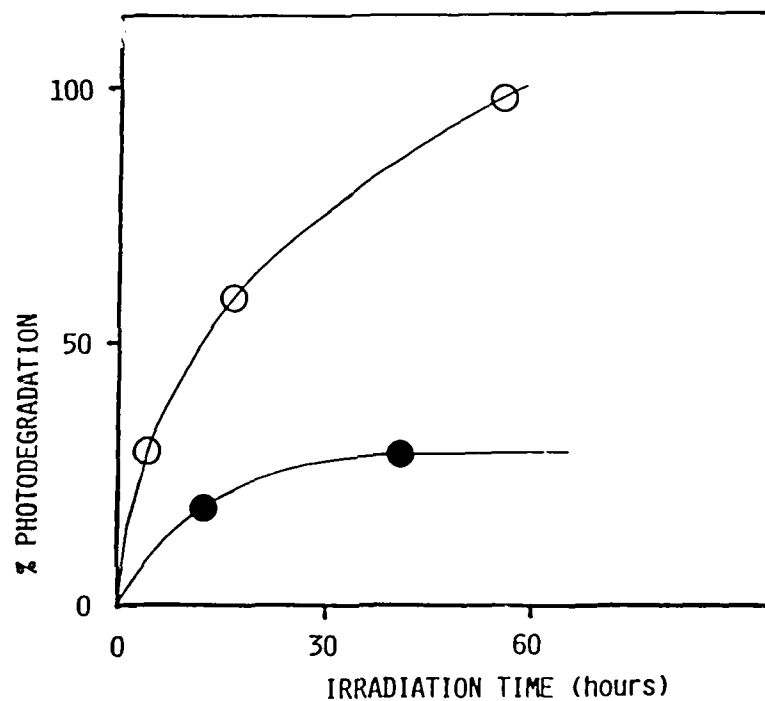
Fig 9 —

Photocatalytic degradation of BE with organic conducting polymer. Spontaneous photodegradation

(●) and over 30% iodine doped PPA membrane, 8.6 cm^2 surface area (○). BE initial concentration 2.10^{-3} M, volume 50 mL, spontaneous pH 6.3, irradiation with a 40 watts lamp. Per cent values reported on each curve are corresponding to the highest photodegradation value.
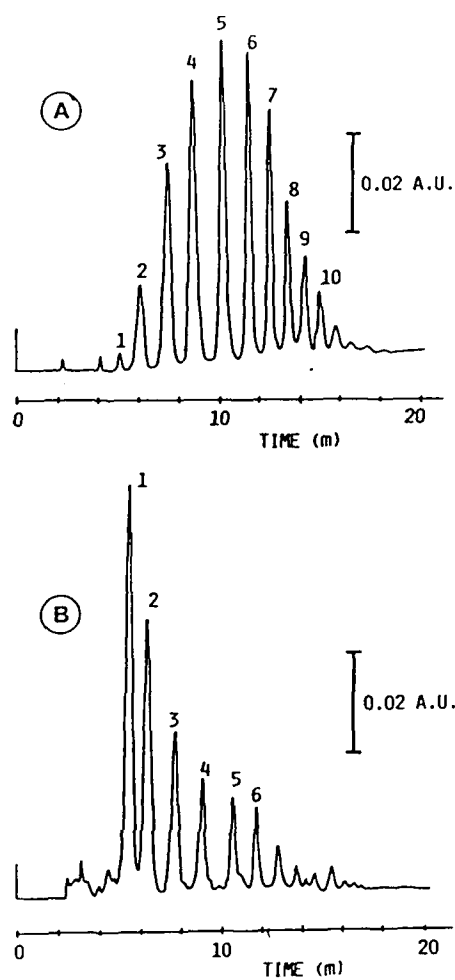
FIGURE 10. Chromatograms before (A) and after 10 minutes of irradiation (B) for IGEPAL CO-520 (6.2 x 10^{-4} M). TiO_2, 2 g L^{-1}. Numbers in figure over each peak represent the number of oxyethylene units.
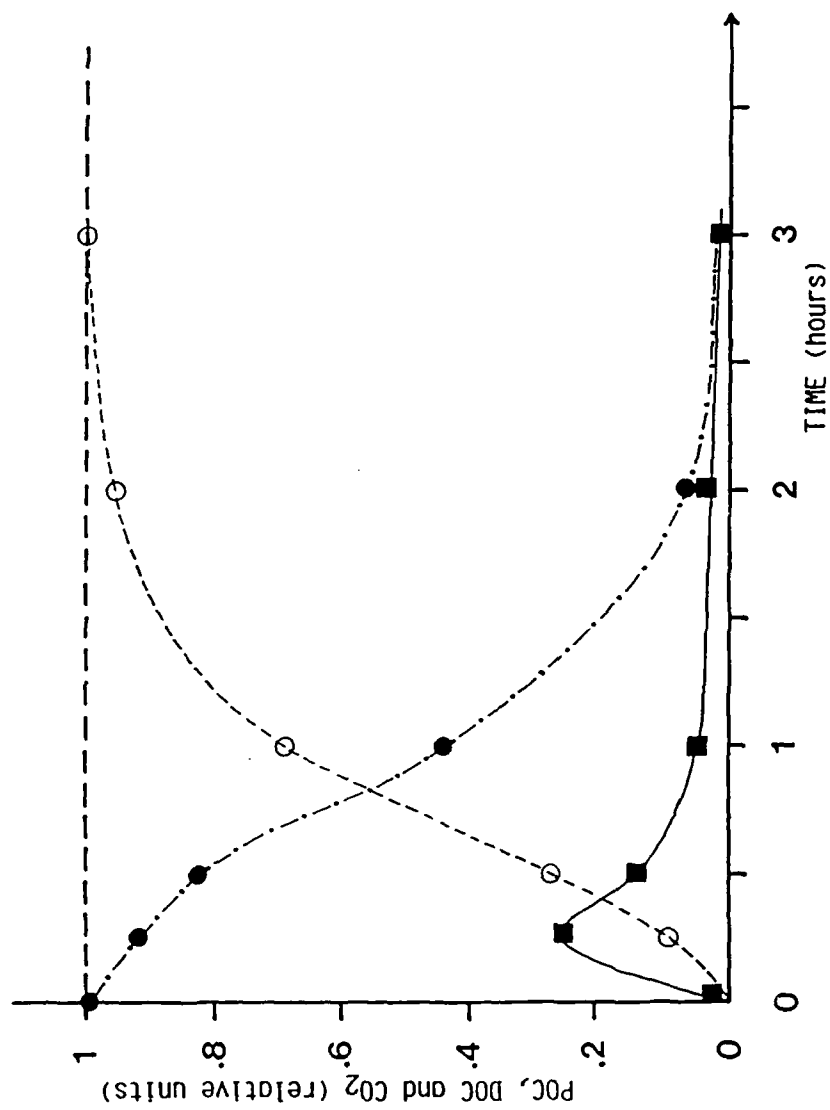
FIGURE 11. CO_2 (○) evolution, DOC (●) and POC (■) variation as a function of irradiation time for IGEPAL CO-720. Units are relative to the stoichiometric value: for CO_2, expected from eq.1; for DOC and POC relative to total carbon. Experimental conditions as in Fig.1 .
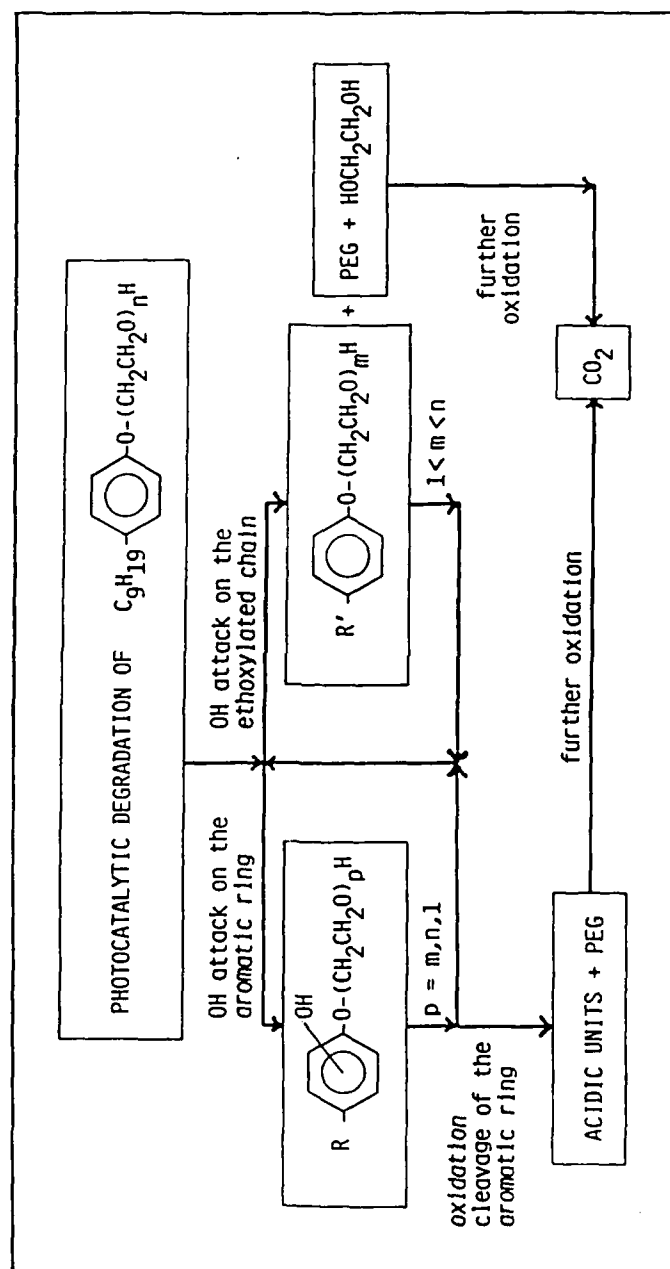
FIGURE 12. Photodegradation routes for NPE's.

Degradation of the aliphatic chain is omitted for clarity.

5
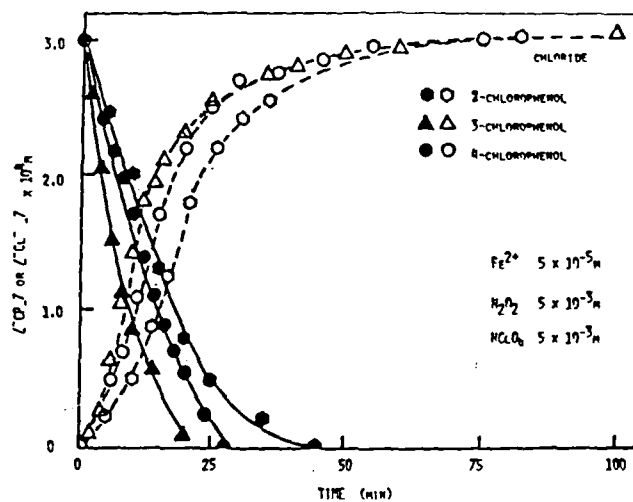
6
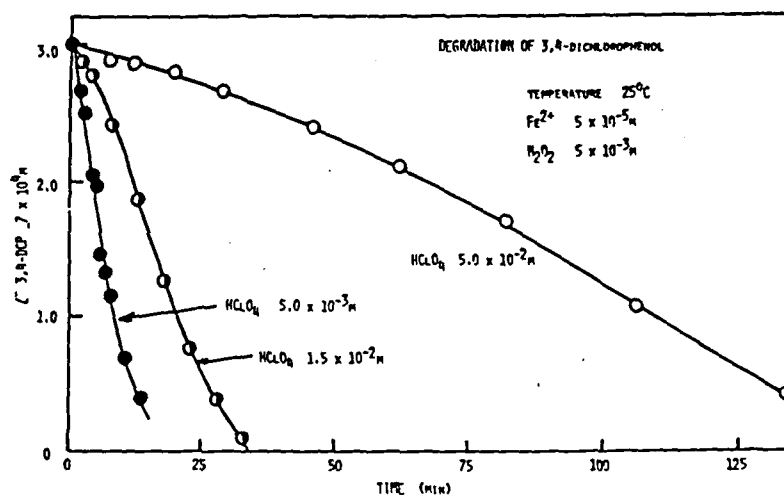
Figure 13 Degradation of monochlorophenols by Fenton's
reagent and concomitant appearance of free chloride
ions.

Figure 14 Disappearance of 3,4-DCP as a function of time at
different $HClO_4$ concentrations.
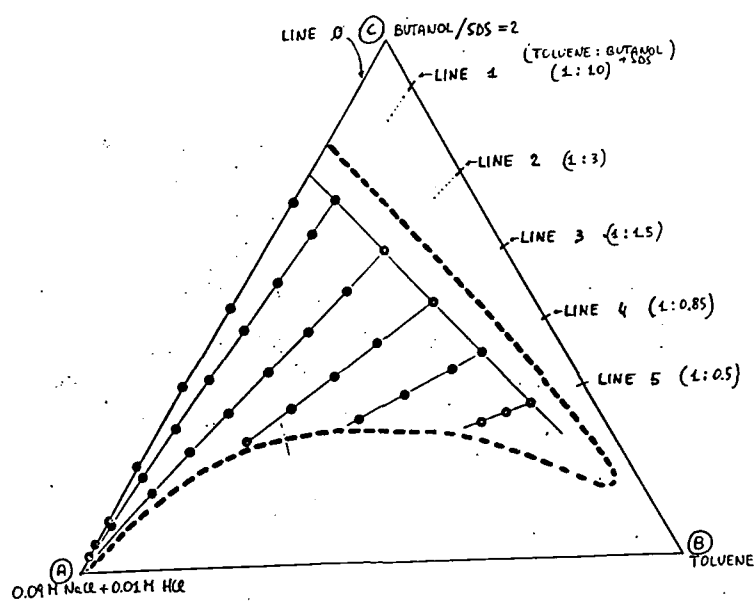
Figure 15 Pseudoternary phase diagram of the system
water(0.09 M NaCl + 0.01 M HCl) - toluene -
(1-butanol:SDS = 2:1), showing the single-phase
at 25 C. The straight lines represent the dilution
lines by water and the points the microemulsion
compositions at which the kinetic runs were
performed
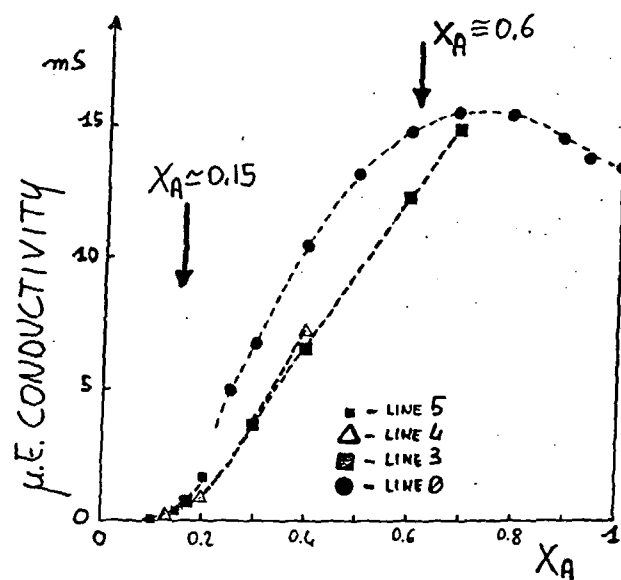
Figure 16 Conductance of a series of microemulsions, according to the lines shown in Fig. 7
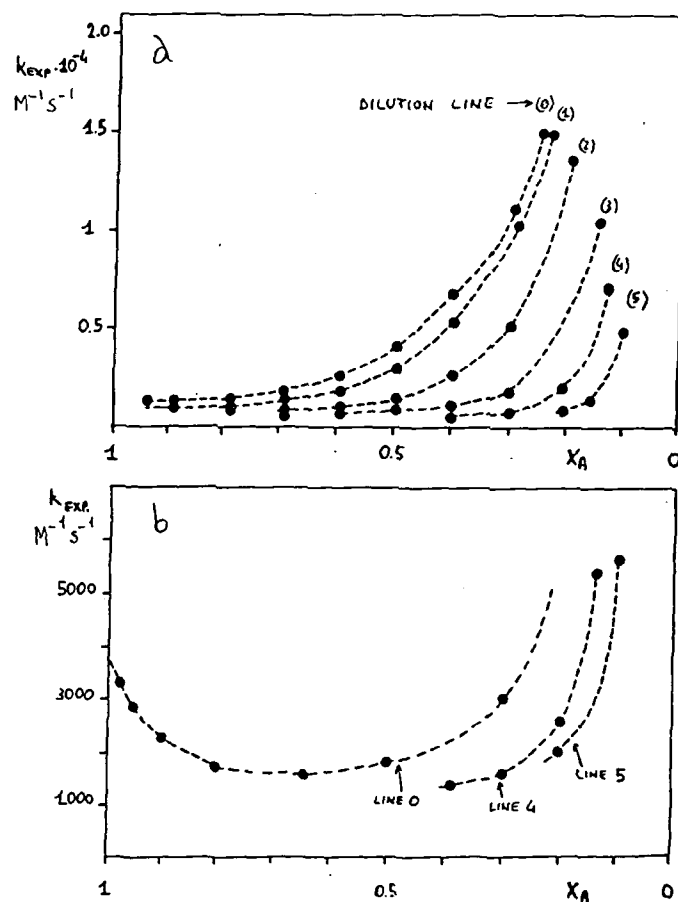
Figure 17 Experimental rate constants for the oxidation
of catechols by $IrCl_6^{2-}$ in microemulsions
(for the dilution lines see Fig. 7)
(a) di-t-butylcatechol (b) catechol
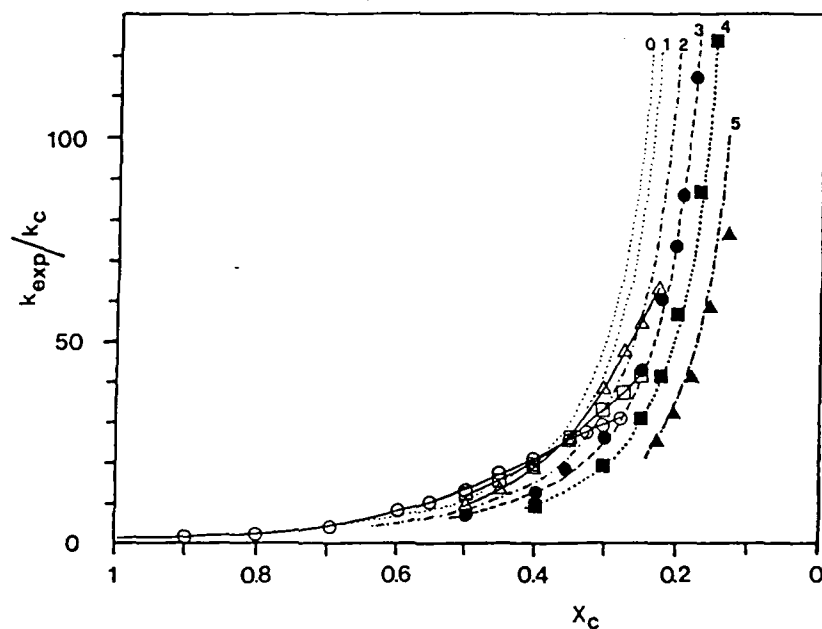
FIG.48: Experimental (points) and calculated (dashed and dotted lines) rate constants in microemulsion for dilution lines 0-5, versus the aqueous weight fraction X_C. Dilution line 0 = ($\bigcirc$), dilution line 1 = ($\square$), dilution line 2 = ($\triangle$), dilution line 3 = ($\bullet$), dilution line 4 = ($\blacksquare$), dilution line 5 = ($\blacktriangle$). The fit curves are calculated with the following parameters in eq.(24): $P_{wi}^A = 0.15$, $P_{wo}^A = 0$, $P_{wi}^B = 0.02$, $P_{wo}^B = 0$, where $A = IrCl_6^{3-}$ and $B = CoW_{12}O_{40}^{5-}$.
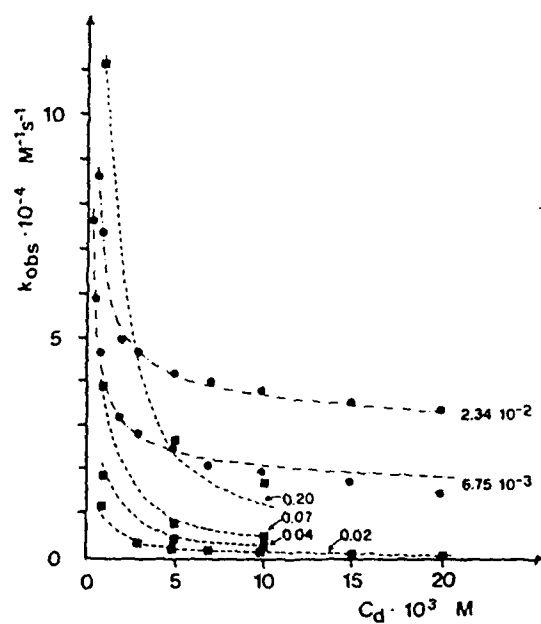
Figure 19.Second-order rate constant (L mol^{-1} s^{-1}) observed as function of the surfactant concentration at fixed added salt: (●) Na$_2$SO$_4$; (■) NaCl. Concentrations of the added salt are indicated. Dashed lines refer to the behavior calculated according to eq 18.
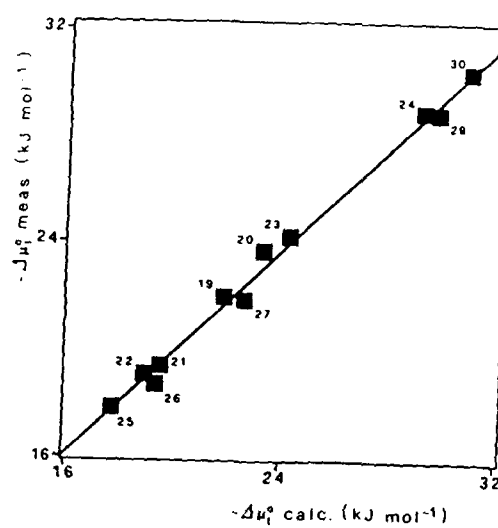
Fig. 20

Comparison between calculated and measured
free energies of transfer of polysubstituted
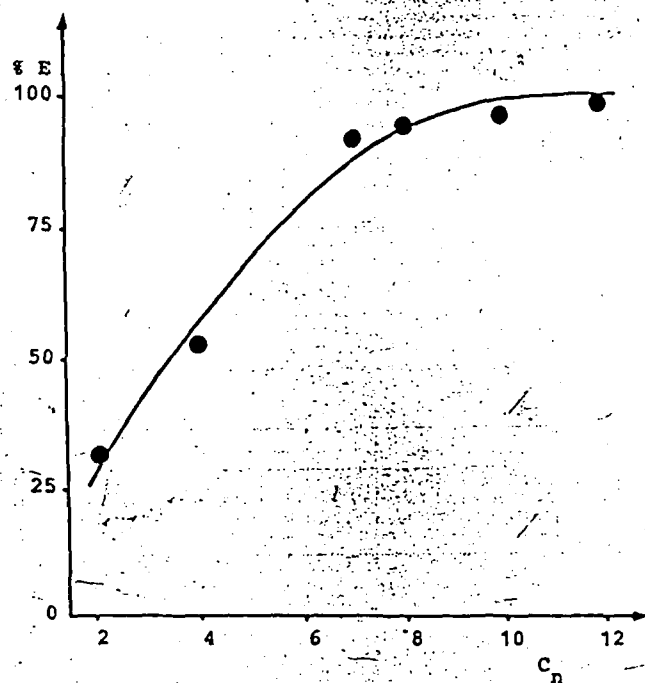phenols (correlation coefficient 0.996)

Figure 21 Plot of the percent extraction of iron (III)
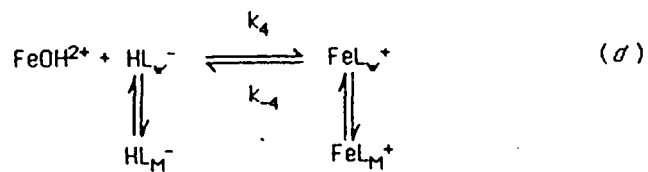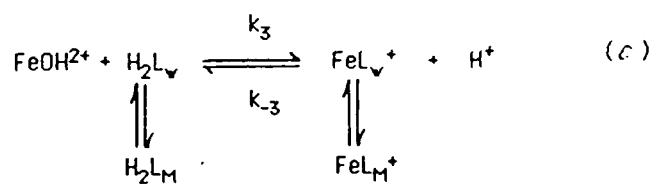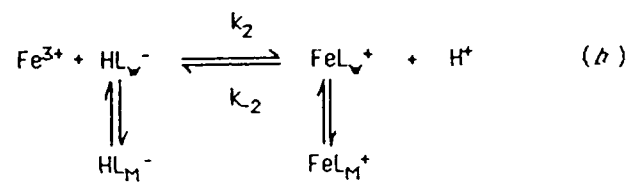as a function of ligand alkyl chain length.

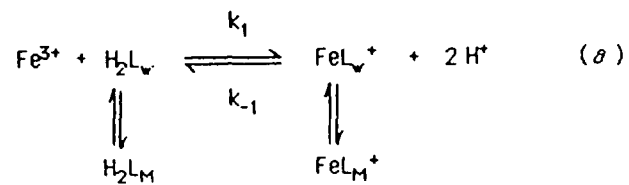$$Fe^{3+} + H_2L_w \underset{k_{-1}}{\overset{k_1}{\rightleftharpoons}} FeL_w^+ + 2H^+ \qquad (a)$$

$$H_2L_M \qquad\qquad FeL_M^+$$

$$Fe^{3+} + HL_w^- \underset{k_{-2}}{\overset{k_2}{\rightleftharpoons}} FeL_w^+ + H^+ \qquad (b)$$

$$HL_M^- \qquad\qquad FeL_M^+$$

$$FeOH^{2+} + H_2L_w \underset{k_{-3}}{\overset{k_3}{\rightleftharpoons}} FeL_w^+ + H^+ \qquad (c)$$

$$H_2L_M \qquad\qquad FeL_M^+$$

$$FeOH^{2+} + HL_w^- \underset{k_{-4}}{\overset{k_4}{\rightleftharpoons}} FeL_w^+ \qquad (d)$$

$$HL_M^- \qquad\qquad FeL_M^+$$

Fig. 22
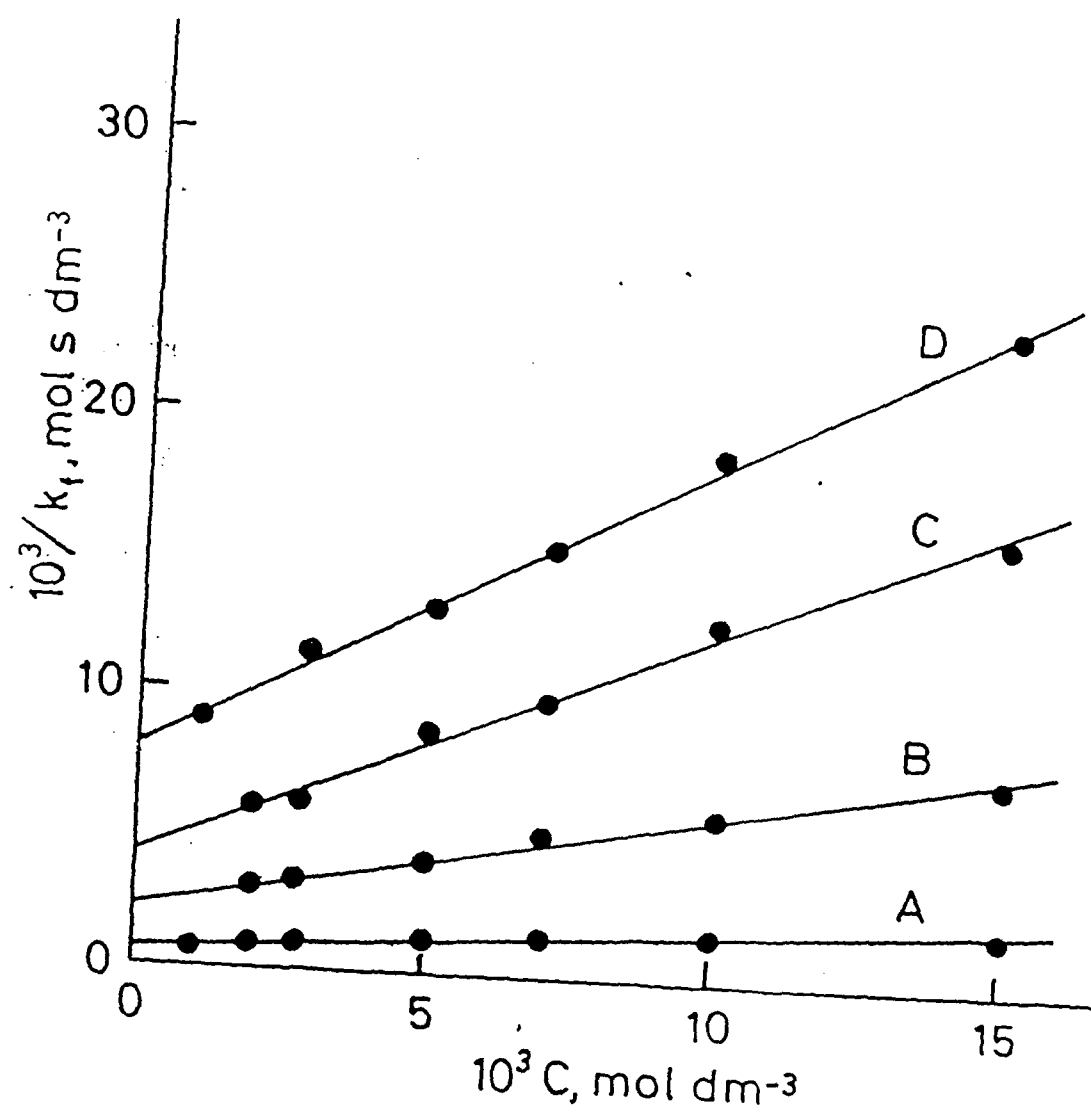
Fig. 23

Plots of $1/k_f$ against C for ligand PAS-C$_2$ at $[H^+] = 1.67 \times 10^{-2}$ (A), 3.87×10^{-2} (B), 6.06×10^{-2} (C), and 11.3×10^{-2} mol dm^{-3} (D).
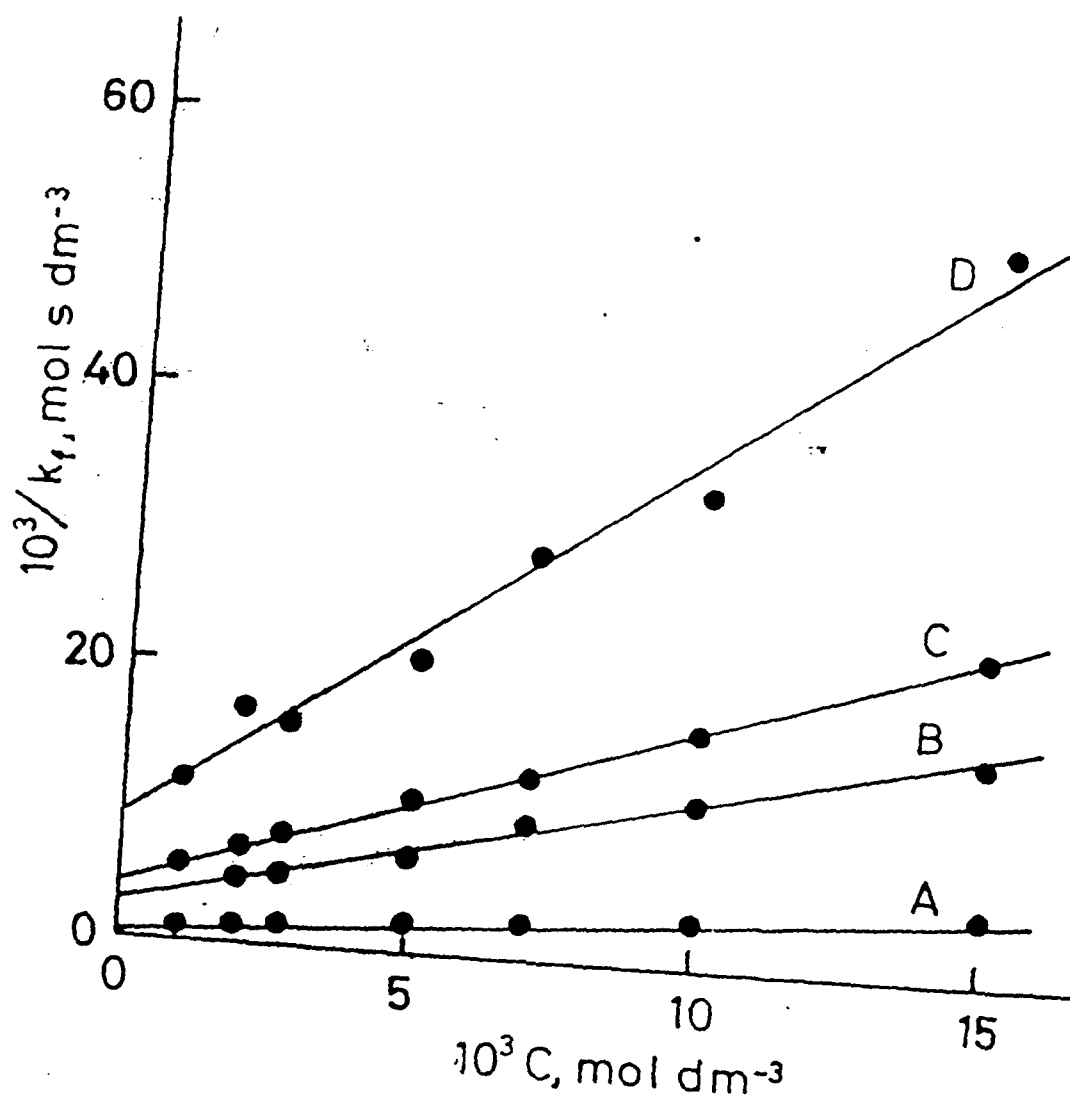
Fig. 24
Plots of $1/k_f$ against C for ligand PAS-C$_4$ at [H$^+$] = 1.74×10^{-2}
(A), 4.38×10^{-2} (B), 6.42×10^{-2} (C), and 11.3×10^{-2} mol dm^{-3}
(D).